

**Stability and Control of
Two-Dimensional Biped Walking**

Tad McGeer

CSS-IS TR 88-01

STABILITY AND CONTROL OF TWO-DIMENSIONAL BIPED WALKING

Tad McGeer*
Simon Fraser University
Burnaby, British Columbia, Canada V5A 1S6

18 September 1988

Abstract

Human-like walking is a natural dynamic mode of a pair of coupled pendula. The mode is most easily excited by descending a shallow slope, but energy can be added and removed in several other ways to allow walking over a range of up- and downhill grades. Leg geometry and mass properties can be adjusted within generous limits, a torso can be added, and a degree of jostling tolerated without upsetting the natural limit cycle. The cycle can also be modulated to vary footfalls from one step to the next, while maintaining a fluid and efficient walking rhythm.

*School of Engineering Science. (TMCG@SFU.MAILNET, Tad.McGeer@cc.sfu.ca)

Symbols
(Defining equations are notes in parentheses)

Roman

A	linear system matrix (115)	\bar{h}	coefficient of γ in S-to-S equations (26), (43)
a	impulse application point	I	identity matrix
\bar{a}_T	derivative of static equilibrium <i>w.r.t.</i> torso angle (91), (45)	I	moment of inertia
\bar{a}'	coefficient of θ_T^* in S-to-S equations (68)	K	stance stiffness matrix (84)
B	coefficient of E, ϵ in S-to-S equations (44), (68)	k_T	torso controller gain (49)
\bar{b}	derivative of static equilibrium <i>w.r.t.</i> slope (6), (86)	L	coefficient of \bar{P} in S-to-S equations (43)
C_T	stance damping matrix (57)	l	leg length (fig. 7)
c	distance from foot to leg mass centre (fig. 7)	M	stance inertia matrix (78), (89)
$D_{\theta\theta},$	submatrices of start-of-step to	M_0	legs-vertical inertia matrix (4)
$D_{\theta\Omega},$	end-of-step transition matrix	m	mass (fig. 7)
$D_{\Omega\theta},$	(7), (8), (116)	\bar{P}	toe-off impulse
$D_{\Omega\Omega}$		P	magnitude of toe-off impulse (120)
D'	(20)	\bar{p}	toe-off impulse of unit magnitude (120)
E	energy input by toe-off pulsing (32)	Q	matrix of eigenvalues (116)
F	support-transfer index exchanger (12), (62)	R	foot radius (fig. 7)
\bar{f}	step-to-step function (22)	\bar{r}	position vector
G	derivative of velocity <i>w.r.t.</i> $\bar{\Omega}$ (34)	r_{gyr}	radius of gyration
g	gravitational acceleration (fig. 7)	S	step-to-step transition matrix (26), (43)
H	angular momentum	s	stride length
\mathcal{H}	angular impulse	T	torque
		V	linear velocity
		w	offset from leg axis to leg mass centre (fig. 7)
		z	eigenvalue of step-to-step equations (26)

Greek

α	leading leg angle at support transfer (13)
Γ_a	impulse-coupling matrix (35)
γ	slope (fig. 7)
$\Delta\theta$	change in θ from reference position
ζ_T	torso controller damping ratio (51)
ϵ	angle of \vec{p} w.r.t. trailing leg (120)
θ	angle relative to surface normal (fig. 7)
$\Delta\vec{\theta}_{SE}$	static equilibrium position (6), (60)
$\Delta\vec{\theta}_W$	derivative of $\Delta\vec{\theta}_{SE}$ w.r.t. w (85)
Λ	support transfer matrix (14), (100)
$\vec{\lambda}$	angle vector at support transfer (11)
τ	dimensionless time $t\sqrt{g/l}$
τ_T	damping time constant of torso controller (49)
Φ	matrix of eigenvectors (116)
Ω	angular speed
ω	angular frequency

Sub- and superscripts

*	including active torso control
+	immediately before support transfer
-	immediately after support transfer
0	steady cycle conditions
C	stance leg
e	constant-energy step-to-step pulsing
F	swing leg
g	due to gravity
H	at the hip
k	step index
P	passive walking
SE	static equilibrium
T	torso

1 Passive stability in walking

Whenever possible, each of us tries to avoid falling asleep while standing up. We know that standing is statically unstable, so we must stay awake to maintain balance. It would seem, therefore, that since active stabilisation is required just to keep a biped standing still, it should also be necessary to sustain walking. But surprisingly enough this is not always true. For some bipeds, walking is a naturally stable limit cycle; thus such systems are *statically* unstable but *dynamically* stable. We will discuss the physics involved, and how it can be exploited to achieve dextrous and efficient walking.

As we shall explain, passively stable gaits compare reasonably well with those of humans, so the analysis offers some useful insight for kinesiology. However, our own emphasis is on design of bipedal machines. We know of at least a dozen research efforts in this area; reports include those of [Lee 88], [Mita 84], [Miura 84], [Raibert 86], [Takanishi 85], [Yamada 85], and [Zheng 88]. These cover a remarkable variety of approaches, but in each case the research focus, and the principle impediment to early practical use, is active generation and stabilisation of the gait. In our view the alternative path of passive stability facilitates understanding and simplifies design.

Our approach is very much influenced by a background in aircraft design, which offers a useful historical analogy. The development of fixed-wing aircraft began with work on gliders. First steady-state gliding was understood (beginning with Sir George Cayley in the early 1800's [Gibbs-Smith 70]). Inherent stability was also considered: gliders were and are designed so that disturbances excite only a brief transient, after which steady flight is naturally reestablished. Once efficient and stable designs were found, controls for changing speed and direction were developed (by Otto Lilienthal, the Wright Brothers, and others). Finally, a powerplant was added to sustain level flight and climbs, which by that time involved only a small modification to the original glider design.

The appeal of this approach is that it allowed progress in an orderly fashion, with each step involving a system no more complicated than necessary to address the next problem at hand. We have applied the same approach to walking. Thus we began with a "biped glider" (*i.e.* powered by walking downhill). The theory and experimental results were reported in [McGeer 88]. Here we present a "powered" model, which allows for walking on shallow rolling slopes, and for varying step length from stride to stride. Still it remains incomplete: we restrict attention to walking in 2D, and we exclude steep up- and downhill grades, such as stairways. However we expect that these can eventually be accommodated.

There are several options for adding power and control to the passive walking model. We will consider the following four: torque application between legs (*i.e.* at the hip joint), torque on the stance leg only, leg length modulation, and impulse application on the trailing leg as it leaves the ground. We will first consider a pair of legs without

a body, and later study the effect of a torso. Our criteria for evaluation are inherent stability over a range of slopes and stride lengths, weight-specific resistance (the most fundamental measure of efficiency), and ease of mechanical design. In our view the best performance is realised by a combination of stance leg torquing for going downhill and toe-off pulsing for going uphill; we are now designing a machine to test these methods.

Discussion here begins with a brief review of gravity-powered walking, including results from our experiments, and review of a model which explains the dynamics of walking with a minimum of analysis. We will then develop more comprehensive mathematics and apply it to a variety of examples.

2 Review of gravity-powered walking

The most elegant example of a gravity-powered biped is the toy sketched in figure 1. It is wonderfully simple and fully passive. However, its motion is somewhat complicated by coupling of the longitudinal cycle with side-to-side rocking, which it uses to clear the swing foot on each step. As a dynamical simplification we built a two-dimensional version as shown in figure 2. It is comparable to a person on crutches, having paired outer legs alternating with a broad-footed centre leg. This arrangement constrains the motion to the longitudinal plane. Swing foot clearance is no longer by passive wobbling, but rather by active intervention of small motors in each leg. But apart from the retraction mechanism the legs are rigid, and the only other moving part is a free pin joint at the hip. The feet are semicircular and have rubber soles.

Figure 3 illustrates the behaviour of the test machine. We start it by hand on a shallow slope, in this case 2.5%. After a few steps it settles into a reasonably steady gait, with some characteristic step period and step length. Figure 4 compares experiment with prediction over a range of slopes. The agreement is reasonably good, so we can have some faith that the analytical model is a sound basis for further work.

The data of figure 4 can also be compared with human walking. For such comparisons dimensionless units are particularly convenient; thus our analysis throughout is cast with total mass m , leg length l , and gravity g providing the base units. Hence the unit of time is $\sqrt{l/g}$, and the step length is measured by the angle α of the leading leg. In some casual experiments with a 75cm toddler and a 195cm adult, we found $\tau_0 \approx 2$ for each in a comfortable gait, with $\alpha_0 \approx 0.3$. For the same stride length in figure 4, $\tau_0 \approx 2.8$. τ_0 values closer to those for a human can be achieved with different machine parameters (as in figure 9) which suggests that man and machine exploit the same dynamics, at least to first order.

Another result from figure 4 is the fundamental efficiency of walking. Different modes of transport are often compared by specific resistance, *i.e.* mean “drag” force normalised by weight. The classic comprehensive comparison is by [Gabielli 50]. For a gravity-

powered vehicle the resistance is just equal to the steady-state descent angle, and so about 0.025 for our test machine walking with $\alpha_0 = 0.3$. This compares favourably with an aircraft or high-speed boat, and would be still lower, perhaps by a factor of two, if the machine had a massive torso (*cf.* figure 9). On the other hand, a specific resistance of 0.01-0.02 is not so good compared with wheeled machines, not to mention the difference in speed. But then one must expect to give up some efficiency in return for going where wheels cannot tread, which is, of course, the *sine qua non* for legged locomotion.

3 The synthetic wheel

To understand the dynamics of passive walking, consider a “synthetic wheel”: a machine like ours but with parameters chosen for analytical simplicity. As shown in figure 5, it has a large mass at the hip, which effectively prevents swinging of the free leg from accelerating the stance leg. It also has feet with radius equal to the leg length, which reduces the stance leg to nothing more than a spoke in a wheel. So like a wheel the stance leg will roll at constant speed along a flat surface, as plotted in figure 6.

Meanwhile, since the hub of the wheel travels at constant speed, the free leg reduces to an ordinary unforced pendulum swinging sinusoidally at its natural frequency. So (provided that the swing foot is kept clear of the ground) a step can proceed as in figure 6. The cycle rolls along like an ordinary wheel, and in the absence of friction would have zero specific resistance.

For practical use one would prefer a machine with smaller feet and more flexibility in the mass distribution. The general arrangement sketched in figure 7 covers a wide range of design options. Of course the motion of such a system is somewhat more complicated than that of the synthetic wheel, and there is some specific resistance. With $R < 1$ energy is lost at each support transfer, by the same mechanism that causes a wobbling domino to lose energy as it rocks from edge to edge. Nevertheless the synthetic wheel provides a first-order approximation for the walking cycle (*cf.* figures 6, 20). In particular, it predicts the period of one step, which can be calculated by matching start and end conditions for the two legs, as follows.

The stance leg rotates at constant speed, so

$$\theta_C(\tau_0) = \alpha_0 = -\alpha_0 + \Omega_C \tau_0 \quad (1)$$

Meanwhile the swing leg moves sinusoidally, so that

$$\theta_F(\tau_0) = -\alpha_0 = \alpha_0 \cos \omega_F \tau_0 + \frac{\Omega_C}{\omega_F} \sin \omega_F \tau_0 \quad (2)$$

Combining these leads to the conclusion that

$$\omega_F \tau_0 = 4.058 \quad (3)$$

By comparison ω_F for our machine turns out to be 1.39; thus $\omega_F\tau_0 = 3.89$ at $\alpha_0 = 0.3$. The synthetic-wheel approximation leaves only a 4% error.

Notice also that τ_0 for the synthetic wheel does not depend on α_0 . Thus to change the forward speed one adjusts not the cadence (except to the extent that the pendulum frequency decreases for large α_0) but rather the amplitude of each step. Figure 4 shows that this is quite a good approximation for our machine, and it also applies to people; changing speed by a factor of three changes τ_0 by only a few percent.

Thus a machine of the type shown in figure 7 exploits much the same effect as sustains a synthetic wheel. However, it is expressed in a more elaborate mathematical form, which we will now develop.

4 Analytical procedure

The walking cycle has two phases: stance and support transfer. Each phase has a corresponding set of equations. The stance equations allow one to jump mathematically between the support-transfer times in figure 6. Thus given the leg angles $\vec{\theta}$ and speeds $\vec{\Omega}$ just *after* support transfer on step k , one can calculate $\vec{\theta}$ and $\vec{\Omega}$ just *before* support transfer on step $k + 1$. The support transfer equations then give the change in $\vec{\Omega}$ on heel strike, which we model as impulsive and inelastic. (Results such as those in figure 4 indicate that the impulsive approximation is quite good for the hard surfaces on which our experiments have been done, although for large α_0 leg bending dynamics do become noticeable.) Putting stance and support transfer together produces a set of 4 nonlinear step-to-step (S-to-S) equations, relating $(\vec{\theta}, \vec{\Omega})$ at the start of steps k and $k + 1$. Requiring repetition from step-to-step then produces the steady-cycle conditions.

Existence of a steady cycle for an arbitrary choice of slope and machine parameters is by no means guaranteed, but it turns out that cycles do exist over a broad range of conditions. When a cycle is found, the next issue is stability. We address this issue by linearising the S-to-S equations for small perturbations on the steady cycle, and then applying standard stability analysis for linear systems. These linearised equations are useful not only for studying transient behaviour, but also for analysis of candidate control laws.

If the gait is found to be stable for small perturbations, the next question is, "how small is small?" There is certainly a limit: obviously if the machine is released from rest with legs vertical, it will topple over rather than walk. Some guidelines for the allowable range of perturbations emerge from our examples, but in general one must find the answer by numerical solution of the nonlinear S-to-S equations.

We begin by developing walking equations for a "basic biped," and later add terms for toe-off pulsing and a torso.

5 Stance dynamics

The equations of motion for the biped during stance are derived in appendix B. For our purposes at this point only their form is important, namely

$$\mathbf{M}_0 \begin{bmatrix} \Omega_C \\ \Omega_F \end{bmatrix} \equiv \mathbf{M}_0 \dot{\vec{\Omega}} = \vec{T} \quad (4)$$

The general equations are nonlinear, with trigonometric terms in γ and $\vec{\theta}$, and centrifugal terms in $\vec{\Omega}$. But for walking linearisation about legs-vertical is quite justified, since the legs never swing beyond $0.4rad$ of the vertical, and dimensionless speeds always remain small compared with unity. (From figure 6 and (1), the order of Ω is $2\alpha_0/\tau_0$, so about 0.3 at most. In fact walking with Ω approaching unity is impossible; centrifugal effect lifts the stance leg off the ground, and one has to run.)

The RHS of the stance equations (4) includes gravitational torque, and possibly frictional and control torques as well. The gravitational contribution is derived in appendix B; it has the form

$$\vec{T}_g = \mathbf{K}[\Delta\vec{\theta}_{SE} - \Delta\vec{\theta}] \quad (5)$$

Here $\Delta\vec{\theta}$ is the shift from the reference position of $\theta_C = 0$; $\theta_F = \pi$. (Note from figure 7 that θ is measured with respect to the surface normal rather than the vertical.) $\Delta\vec{\theta}_{SE}$ is the static equilibrium position; for small γ it is given by

$$\Delta\vec{\theta}_{SE} = \Delta\vec{\theta}_W + \vec{b}\gamma \quad (6)$$

If the foot radius is zero, and the mass centres are on the leg axes, then for equilibrium both legs must be vertical, and both elements of \vec{b} are -1. If the foot radius is nonzero, then the stance leg must rotate beyond the vertical to put the overall mass centre over the contact point, and $\vec{b}_1 < -1$. $\Delta\vec{\theta}_W$ accounts for any offset between the legs axes and their mass centres.

Additional torque terms due to friction or control application may have a variety of forms; several are treated in our examples. The only condition necessary for convenient analysis is that these terms remain linear in $\vec{\theta}$ and $\vec{\Omega}$. That allows the stance equations (4) to be solved in terms of transition matrices, as reviewed in appendix E:

$$\Delta\vec{\theta}(\tau_k) = \mathbf{D}_{\theta\theta}[\Delta\vec{\theta}_k - \Delta\vec{\theta}_{SE}] + \mathbf{D}_{\theta\Omega}\vec{\Omega}_k + \Delta\vec{\theta}_{SE} \quad (7)$$

$$\vec{\Omega}(\tau_k) = \mathbf{D}_{\Omega\theta}[\Delta\vec{\theta}_k - \Delta\vec{\theta}_{SE}] + \mathbf{D}_{\Omega\Omega}\vec{\Omega}_k \quad (8)$$

With this set of transition equations one can compute the conditions at the end of the k^{th} step given the step period τ_k and start-of-step conditions $\Delta\vec{\theta}_k$ and $\vec{\Omega}_k$.

6 Support transfer

Next the support transfer equations must be invoked to get from the end of step k to the start of step $k + 1$. The event is approximated as an instantaneous exchange of support just as the swing foot hits the ground. The forward leg's angle at that instant is defined to be $-\alpha_k$, and the rear leg's angle satisfies

$$(l_F - R) \cos \Delta\theta_F = (l_C - R) \cos \alpha_k \quad (9)$$

Most simply, $\cos \Delta\theta_F = \cos \alpha_k$ with matched legs, but in general we write

$$\Delta\vec{\theta}_k = \vec{\lambda} \alpha_k \quad (10)$$

where

$$\vec{\lambda} = \begin{bmatrix} -1 \\ \Delta\theta_F/\alpha_k \end{bmatrix} \quad (11)$$

Notice that since $\Delta\vec{\theta}$ is defined with respect to the surface normal, $\vec{\lambda}$ is independent of γ . On this point it is also worth noting that if one were interested in stairs rather than a smooth slope, then γ would be zero, and the height change would appear as a modification to $\vec{\lambda}$.

At support transfer the legs exchange roles, and so the indices of $\vec{\theta}$ are flipped. Thus define the "flip" matrix \mathbf{F} ,

$$\mathbf{F} \equiv \begin{bmatrix} 0 & 1 \\ 1 & 0 \end{bmatrix} \quad (12)$$

Then

$$\Delta\vec{\theta}_{k+1} = \vec{\lambda} \alpha_{k+1} = \mathbf{F}\Delta\vec{\theta}(\tau_k) \quad (13)$$

So much for the change in leg angles at support transfer, which is just a matter of bookkeeping. The change in leg speeds, on the other hand, involves some physics. Conservation of angular momentum holds for the whole system about the point of collision, and for the trailing leg about the hip joint. The details are developed in appendix D; again only the form of the equations is required for present purposes, namely

$$\vec{\Omega}_{k+1} = \mathbf{\Lambda}\vec{\Omega}(\tau_k) \quad (14)$$

The matrix $\mathbf{\Lambda}$ is a function of α at the instant of support transfer. It also incorporates the "flip" matrix to exchange leg indices.

7 Nonlinear step-to-step equations

Putting the stance transition equations (7), (8) together with the support transfer conditions (13), (14) produces the step-to-step equations:

$$\vec{\lambda} \alpha_{k+1} = \mathbf{F} \left(\mathbf{D}_{\theta\theta} [\vec{\lambda} \alpha_k - \Delta \vec{\theta}_{SE}] + \mathbf{D}_{\theta\Omega} \vec{\Omega}_k + \Delta \vec{\theta}_{SE} \right) \quad (15)$$

$$\vec{\Omega}_{k+1} = \Lambda \left(\mathbf{D}_{\Omega\theta} [\vec{\lambda} \alpha_k - \Delta \vec{\theta}_{SE}] + \mathbf{D}_{\Omega\Omega} \vec{\Omega}_k \right) \quad (16)$$

These are nonlinear, since Λ is a function of α_{k+1} , and τ_k is a function of α_k and $\vec{\Omega}_k$.

8 Solution for the walking cycle

If a steady cycle exists, then initial conditions will repeat from step to step:

$$\alpha_{k+1} = \alpha_k = \alpha_0 \quad (17)$$

$$\vec{\Omega}_{k+1} = \vec{\Omega}_k = \vec{\Omega}_0 \quad (18)$$

One can impose these conditions on the S-to-S equations (15), (16), and derive a compact solution for the steady cycle. First, solve for $\vec{\Omega}_0$ using (16):

$$\vec{\Omega}_0 = [\mathbf{I} - \Lambda \mathbf{D}_{\Omega\Omega}]^{-1} \Lambda \mathbf{D}_{\Omega\theta} [\vec{\lambda} \alpha_0 - \Delta \vec{\theta}_{SE}] \quad (19)$$

Then substitute for $\vec{\Omega}_0$ in (15); the end result can be written as follows. Define

$$\mathbf{D}'(\alpha_0, \tau_0) = \mathbf{D}_{\theta\theta} + \mathbf{D}_{\theta\Omega} [\mathbf{I} - \Lambda \mathbf{D}_{\Omega\Omega}]^{-1} \Lambda \mathbf{D}_{\Omega\theta} \quad (20)$$

Then (15) can be written as

$$\begin{aligned} \vec{0} &= [\mathbf{D}' - \mathbf{F}] \vec{\lambda} \alpha_0 - [\mathbf{D}' - \mathbf{I}] \Delta \vec{\theta}_{SE} \\ &= [\mathbf{D}' - \mathbf{F}] \vec{\lambda} \alpha_0 - [\mathbf{D}' - \mathbf{I}] [\Delta \vec{\theta}_W + \vec{b}\gamma] \end{aligned} \quad (21)$$

The last line follows from (6). This is the steady-cycle condition. Any one of α_0 , τ_0 , or γ can be specified as the independent variable. Usually we specify α_0 . (21) then has either two solutions or none. If two, then one cycle has $\omega_F \tau_0 < \pi$, and is invariably unstable. The other corresponds to a synthetic-wheel-like cycle (figure 6 and (3)) with $\omega_F \tau_0$ between π and $3\pi/2$. This is the solution of interest, and since (21) is nonlinear in τ_0 , we search for it by Newton's method. The synthetic-wheel estimate for τ_0 (3) is obviously a good starting point, and *if* a solution exists, convergence requires about 5 iterations.

9 Linearised step-to-step equations

Once a steady cycle is found, the question of stability arises. To address this question, it is perhaps best to think of the S-to-S equations (15), (16) in the form

$$\vec{f}(\tau_k, \alpha_{k+1}, \vec{\Omega}_{k+1}, \alpha_k, \vec{\Omega}_k, \gamma, \dots) = \vec{0} \quad (22)$$

One could add more variables to the argument list of \vec{f} , such as foot radius, leg length, *etc.* However this list is sufficient for the moment. \vec{f} can be expanded in a Taylor series; thus

$$\vec{f}(\tau_k, \alpha_{k+1}, \vec{\Omega}_{k+1}, \alpha_k, \vec{\Omega}_k, \gamma, \dots) \approx \vec{f}_0 + \frac{\partial \vec{f}}{\partial \tau_k} \Delta \tau_k + \frac{\partial \vec{f}}{\partial \alpha_{k+1}} \Delta \alpha_{k+1} + \dots \quad (23)$$

If the reference condition for expansion is the steady cycle, then $\vec{f}_0 = \vec{0}$ (22). So for small perturbations on the steady cycle, the S-to-S equations are

$$\frac{\partial \vec{f}}{\partial \tau_k} \Delta \tau_k + \frac{\partial \vec{f}}{\partial \alpha_{k+1}} \Delta \alpha_{k+1} + \dots \approx \vec{0} \quad (24)$$

In matrix form, this is

$$\nabla \vec{f} \begin{bmatrix} \Delta \alpha_{k+1} \\ \Delta \vec{\Omega}_{k+1} \\ \Delta \tau_k \\ \Delta \alpha_k \\ \Delta \vec{\Omega}_k \\ \Delta \gamma \end{bmatrix} \approx \vec{0} \quad (25)$$

If one knows the conditions at the start of step k , one can use this (and the steady-cycle solution) to predict initial conditions for step $k+1$, and the step period. Thus solving for the unknowns in (25) produces a linear system of the following form:

$$\begin{bmatrix} \Delta \alpha_{k+1} \\ \Delta \vec{\Omega}_{k+1} \\ \Delta \tau_k \end{bmatrix} = \mathbf{S} \begin{bmatrix} \Delta \alpha_k \\ \Delta \vec{\Omega}_k \end{bmatrix} + \vec{h} \Delta \gamma \quad (26)$$

Appendix E develops the terms of this equation in more detail. The advantage of the linear approximation over the exact S-to-S equations (15), (16) is that gait stability can be assessed by a standard eigenvalue calculation. Actually only the upper 3×3 submatrix of \mathbf{S} is needed; the fourth equation in the set, for $\Delta \tau_k$, supplies ancillary information. Thus if the three eigenvalues of (26) have magnitude less than unity, then the walking cycle is stable with respect to small perturbations. (Of course this is the desirable situation, but failing that the linear formulation is helpful for design of a stabilising control law; this was in essence the approach of [Miura 84].)

To avoid any confusion you should recognise that we have gone through two stages of linearisation to reach this point. First, the stance-phase differential equations (4) were linearised about legs-vertical. Their solution was incorporated into nonlinear S-to-S equations (15), (16), which led to solution for the steady walking cycle. Then the S-to-S equations were linearised about this cycle. As I have explained, the stance linearisation is worry-free for walking, but the S-to-S linearisation must be used with due regard for its limited range of validity.

10 Energy input by applying torque to the legs

In [McGeer 88] we used the analysis developed above for extensive calculations of the effects of various parameters – especially R , r_{gyr} , c , w , m_H , and γ – on gravity-powered walking. Here we want to evaluate various strategies for energy input and gait control. The first strategy to investigate is direct torquing of the legs.

Actually there are several options within this category. Torque might be applied at the hip joint, so that the legs react against each other. Alternatively, torque might be applied to the stance leg only, through an ankle joint, or more conveniently by reaction against a leaning torso. A separate issue concerns scheduling the torque during the step. The simplest option is constant torque, in which case the addition to the torque vector in (4) would be

$$\Delta\vec{T} = \begin{bmatrix} T_C \\ 0 \end{bmatrix} \quad \text{for torque on the stance leg} \quad (27)$$

$$\Delta\vec{T} = \begin{bmatrix} T_H \\ -T_H \end{bmatrix} \quad \text{for torque at the hip} \quad (28)$$

These terms work their way into the S-to-S equations (15), (16) through modifications to $\Delta\vec{\theta}_{SE}$. Alternatively, one could vary T in proportion to $\vec{\Omega}$; the effect would be the same as viscous damping and would modify the transition matrix \mathbf{D} . It turns out, however, that viscous torque and constant torque have very similar effects, so the dynamics are apparently not sensitive to the details of the torque schedule.

Hence we offer as representative only a set of constant-torque results. These are plotted in figures 8 and 9. We chose parameters for the example as typical of what is reasonable in a walking machine. $\alpha_0 = 0.3$ is a comfortable stride for human walking. $R = 0.4$ is a good balance between the high efficiency and forgiving dynamics obtained with large feet (as in a synthetic wheel) and the small footprint of small feet (which a practical machine would need to climb stairs). r_{gyr} and c are not terribly critical. m_H is a point mass at the hip, which roughly represents the effect of putting a torso on top of the legs; more rigorous analysis is done later in the paper. Note that the specific

resistance (*i.e.* slope for $T = 0$) with $m_H = 0.7$ is only half that with $m_H = 0$; the higher overall mass centre reduces the loss at support transfer.

Focus attention now on figure 9, whose message, in summary, is this: stance torque is effective for going downhill but not uphill. On the other hand, hip torque is more effective for going uphill than downhill, but it really isn't very helpful in either direction. Some explanation is required to decipher this message from the plot. First note that each curve comes to an abrupt end in the midst of the figure. Beyond these points there is no steady walking cycle, *i.e.*, no solution to (21). The plots of step period show that vanishing of the steady cycle corresponds to τ_0 reaching some minimum permissible value. In fact this minimum value is close to but somewhat larger than $\omega_F \tau_0 = \pi$, or by comparison with figure 6, time for only half a swing leg cycle during the step. Hence the cycle vanishes because the stance leg topples forward more quickly than the free leg can swing through.

As τ_0 increases from this minimum value, there is a range over which all three eigenvalues of the S-to-S equations (26) are smaller than unity. (Only the largest is plotted as $|z|$.) But then there is a transition to instability, which is perhaps less malignant than complete vanishing of the walking cycle, but still quite unwelcome. In fact, as later examples show, the limited range of desirable τ_0 indicated by figure 9 is common to all strategies for energy input. Thus half the battle in steady powered walking – and in step-to-step gait variation – is to keep the step period in this range.

Before proceeding further I should make a couple of notes about figure 9, so that its main message is not obscured by odd details. First, while it is intuitive that negative stance torque should slow down the step, the opposite effect of hip torque may be surprising. The explanation is that negative hip torque not only decelerates the stance leg, but also reduces the swing amplitude. This causes “earlier” heel strike, and so reduces τ_0 . Other features which catch the eye are the kinks in the plots of stability index. (The kinks are somewhat more pronounced in later figures.) These leave a misleading impression of some dramatic event; in fact it is just an artifact of plotting only the largest of the three eigenvalues of the S-to-S equations (26). The kinks indicate a change in ordering of the eigenvalues; if all three were plotted one would see just two smooth curves intersecting at these points.

The main issue raised by figure 9 now confronts us: torque application to one or both legs allows steady walking over only a limited range of slopes around that for passive walking. Extending this range is a matter of obvious practical interest. As it turns out a simple adjustment is quite effective. We call it w , which means offsetting each leg's mass centre from the axis of the leg. Figure 10 shows that w , like T in figure 9, has a powerful effect on step period and stability. Hence the two parameters can be played against each other to maintain stable walking over a broad range of slopes. This works for both stance torque and hip torque.

These calculations indicating such high sensitivity to w left us quite surprised. There-

fore we checked the calculations against experiment, as plotted in figure 11. The agreement is not completely satisfactory: if we take rolling friction to be -0.007 to match α_0 and τ_0 , then calculations indicate a range of instability whereas tests could be sustained over three 6-foot tables placed end-to-end. On the other hand, if rolling friction is taken to be zero, then we get a better match to the stable w -band, but relatively poor agreement on α_0 and τ_0 . We suspect that the discrepancy arises because support transfer is more complicated than our model specifies, perhaps because of slipping or rebound. Nevertheless the similarity between model and measurement is sufficient to confirm that w is indeed a powerful parameter. Note that the acceptable range of w is only 1% of leg length, or 5mm. That seems remarkably narrow, but in fact it is very perceptible. A few mm makes quite a difference to the feel of manual starting.

11 Step-to-step gait variation

Figures 8, 9, and 10 illustrate walking in *steady state* with various stride lengths. But what about varying stride length from one step to the next? Obviously this is an essential capability for practical legged locomotion, which could be competitive only in places where points of support are intermittent or irregularly spaced. To bring the problem into focus, imagine crossing a (2D) pond via a series of stepping stones. As the foot lands on the k^{th} stone, the position of the next stone is known (and hence the necessary value of α_{k+1}). The question is, what control should be applied to strike it?

Various adjustments could be made to vary the gait from step to step; for the moment consider variations in stance and hip torque. These affect the equilibrium position $\Delta\vec{\theta}_{SE}$, and an appropriate value for $\Delta\vec{\theta}_{SE}$ during the k^{th} step can be calculated from the S-to-S equation (15):

$$\Delta\vec{\theta}_{SEk} = [\mathbf{I} - \mathbf{D}_{\theta\theta}]^{-1} [\mathbf{F}\vec{\lambda} \alpha_{k+1} - \mathbf{D}_{\theta\theta}\vec{\lambda} \alpha_k - \mathbf{D}_{\theta\Omega}\vec{\Omega}_k] \quad (29)$$

If one chooses α_{k+1} and τ_k , then $\Delta\vec{\theta}_{SEk}$ follows. Torque adjustments, in turn, are given by

$$\begin{bmatrix} \Delta T_C \\ \Delta T_H \end{bmatrix} = \begin{bmatrix} \frac{\partial \Delta\vec{\theta}_{SE}}{\partial T_C} & \frac{\partial \Delta\vec{\theta}_{SE}}{\partial T_H} \end{bmatrix}^{-1} [\Delta\vec{\theta}_{SEk} - \Delta\vec{\theta}_{SE0}] \quad (30)$$

Since $\Delta\vec{\theta}_{SE}$ is linear in T_C and T_H , this control is exact so long as the model is perfect.

Of course in practice the model will not be perfect, and so if the control given by (30) were maintained throughout the step one would be left with some error in foot placement. This error could be reduced by evaluating the control law *continuously* throughout the step. That is, use the stance transition equation (7) rather than the S-to-S equation (15) to choose $\Delta\vec{\theta}_{SE}$:

$$\Delta\vec{\theta}_{SE}(\tau) = [\mathbf{I} - \mathbf{D}_{\theta\theta}(\tau_k - \tau)]^{-1} [\mathbf{F}\vec{\lambda} \alpha_{k+1} - \mathbf{D}_{\theta\theta}(\tau_k - \tau)\Delta\vec{\theta}(\tau) - \mathbf{D}_{\theta\Omega}(\tau_k - \tau)\vec{\Omega}(\tau)] \quad (31)$$

The transition matrices are evaluated not for the full step period, but rather for the desired time remaining to heel strike ($\tau_k - \tau$). One must be somewhat careful, since $[\mathbf{I} - \mathbf{D}_{\theta\theta}]$ vanishes as $\tau \rightarrow \tau_k$ and so one will exhaust the control torque if one applies (31) too close to the end-of-step. However, a control law along the lines of (31) will certainly improve foot placement even if used for only part of the step.

Figure 12 offers an example of foot placement control with a perfect model. We imagine scattering stepping stones with spacing varied randomly about a mean value of $\alpha_0 = 0.25$. We select w and a nominal value of T_C to generate a steady walk with $\alpha_0 = 0.25$, $\gamma = 0$, as in figure 10. Walking proceeds across the stones, with ΔT_C , ΔT_H on each step selected according to (29) and (30), while the step period is maintained at the steady-state value. As you can see, precise and dextrous foot placement is possible with quite modest control variations.

The choice of T_C and T_H as stepping-stone control variables is not essential. w is an attractive alternative; values for each leg can be adjusted independently, and small adjustments produce large effects. (In fact, humans may produce similar effects by varying foot shape.) However, formulation of a control law analogous to (30) involves more than just calculating new gradients of $\Delta \vec{\theta}_{SE}$. The problem is that the stance equations treat w as constant; they do not account for *dynamic* changes. To properly formulate a control law for w , one would have to account for the recoil produced by shifting part of the leg mass.

The stepping-stone control law (29) has other applications. In particular, if one wanted to accelerate the natural convergence as shown in figure 3, or to walk in the unstable range of figure 9, then one could set $\alpha_{k+1} = \alpha_0$, $\tau_k = \tau_0$ and simply use (29) as a regulator. The same control law could also be used to maintain an even gait over rolling terrain, *i.e.* with slowly varying γ . (Note, however, that the S-to-S equations as written are not valid for *dynamic* changes in γ . For example, they do not account for the step change in $\vec{\theta}$ – measured from the surface normal – which would occur at a kink in the floor.)

12 Energy input by varying leg length

Return attention now to the problem of steady powered walking. The qualitative idea of the next scheme is to “fake” a downhill grade by leg length adjustment. That is, if the swing leg were shortened relative to the stance leg prior to support transfer, then the effect would be like taking a downhill step. The required length adjustment can be estimated as follows. If γ_P is the slope for passive walking, then

$$mg 2\alpha_0 l (\gamma_P - \gamma) \approx -mg \Delta l \Rightarrow \frac{\Delta l}{l} \approx -2\alpha_0 (\gamma_P - \gamma)$$

energy required
for climbing
energy input by
raising mass centre

For shallow slopes this amounts to no more than a few percent. Such small length changes can be neglected in the stance equations (4) as one can show analytically, or simply by observing that the reference state for linearisation is resting with legs vertical. Changing leg length in that state causes no angular acceleration; hence Δl has no first-order effect. Thus length change enters the analysis only through the support-transfer equations (9) and (14).

The insensitivity of stance dynamics to leg length change is more than just a mathematical simplification. It also means that timing of a length change is not critical; extension of the stance leg, and retraction of the swing leg, need only be sufficiently fast to prevent toe-stubbing in the middle of the step. This is appealing from a practical point of view, as is the fact that retraction actuators are required in any event for foot clearance. Thus we could kill two birds with one set of actuators.

Figures 13 and 14 show the effect of leg length variation, with parameters as in earlier examples. We have made one small change from figures 8 and 9. If α_0 were kept constant, then the step length would vary with Δl . Step length is a more reasonable parameter to fix, so we have adjusted α_0 with Δl accordingly. Figure 13 shows Δl varying with slope just as simple energy analysis suggests. Meanwhile figure 14 shows the effect of length variation on stability. The plots are directly comparable with figure 9 for torque application. Both figures show stable walking over only a limited range of step periods; the ranges indicated by the two figures are almost identical. The corresponding range of feasible slopes in the length-change case is usefully broad with any one value of w , and the range can be extended by varying w , just as in figure 10.

Thus we have two promising options for powered walking, and at this point it is perhaps worthwhile to stop briefly to appreciate the robustness of the walking mode. At first glance a pair of coupled pendula, whose most notable feature of static instability is not obviously helpful, would not seem very likely to walk all by itself. Now it emerges that walking is a natural mode over quite a variety of conditions – which, in fact, we have hardly begun to explore.

13 Energy input by toe-off pulsing

Next we turn to an energy-input strategy which seems quite analogous to human walking. This is to push with the trailing leg as it leaves the ground. Of course an inescapable limitation of this strategy is that it can only be applied for adding energy, which is of no help if one wants to go downhill, *i.e.* $\gamma > \gamma_P$. For the downhill range one could shift the burden to the forward leg, pushing at heel strike. That, however, conveys a powerful

sense of bone-jarring aggravation at the already stressful event of support transfer. A more benign technique of backward leaning of the torso is treated later in the paper.

For analysis of toe-off pulsing the S-to-S equations (15), (16) must be modified to include the energy input, which we approximate as impulsive. This approximation has to be treated with some care, since a true impulse would throw both legs right off the ground. Consequently there is a minimum impulse-application time, set by the condition that the leading foot must maintain a positive contact force. The limit is calculated in appendix G. It turns out to be a small fraction of the step period ($< 0.1\tau_0$), so the impulsive approximation is not bad.

The impulse produces an instantaneous change in $\vec{\Omega}$, which can be calculated by a matrix multiplication analogous to (14). The form is most easily derived from an expression for the energy input, which itself proves quite useful for efficiency and stability calculations. The work done by the impulse is the product of displacement and force, which in the limit is

$$E = \frac{1}{2} [\vec{V}_a^+ + \vec{V}_a^-]^T \vec{P} \quad (32)$$

a denotes the point of application, “-” denotes immediately pre-impulse, and “+” immediately post-impulse. The work done must be equal to the change in kinetic energy, which is

$$E = \frac{1}{2} [\vec{\Omega}^{+T} \mathbf{M} \vec{\Omega}^+ - \vec{\Omega}^{-T} \mathbf{M} \vec{\Omega}^-] = \frac{1}{2} [\vec{\Omega}^+ + \vec{\Omega}^-]^T \mathbf{M} \Delta \vec{\Omega} \quad (33)$$

\vec{V} is proportional to $\vec{\Omega}$, according to an equation of the form

$$\vec{V} = \mathbf{G}_a \vec{\Omega} \quad (34)$$

Thus eliminating \vec{V} in (32) and then solving (33) for $\Delta \vec{\Omega}$ leads to

$$\Delta \vec{\Omega} = \mathbf{M}^{-1} \mathbf{G}_a^T \vec{P} \equiv \Gamma_a \vec{P} \quad (35)$$

Note that \mathbf{M} , \mathbf{G}_a , and Γ_a are functions of $\vec{\theta}$ at the instant of impulse application, which we take to be the start of step.

The effect of the impulse is to modify the initial $\vec{\Omega}$ in the stance equations (7), (8). These now become

$$\Delta \vec{\theta}(\tau_k) = \mathbf{D}_{\theta\theta} [\Delta \vec{\theta}_k - \Delta \vec{\theta}_{SE}] + \mathbf{D}_{\theta\Omega} [\vec{\Omega}_k + \Gamma_a \vec{P}] + \Delta \vec{\theta}_{SE} \quad (36)$$

$$\vec{\Omega}(\tau_k) = \mathbf{D}_{\Omega\theta} [\Delta \vec{\theta}_k - \Delta \vec{\theta}_{SE}] + \mathbf{D}_{\Omega\Omega} [\vec{\Omega}_k + \Gamma_a \vec{P}] \quad (37)$$

The S-to-S equations (15), (16) in turn become

$$\vec{\lambda} \alpha_{k+1} = \mathbf{F} (\mathbf{D}_{\theta\theta} [\vec{\lambda} \alpha_k - \Delta \vec{\theta}_{SE}] + \mathbf{D}_{\theta\Omega} [\vec{\Omega}_k + \Gamma_a \vec{P}] + \Delta \vec{\theta}_{SE}) \quad (38)$$

$$\vec{\Omega}_{k+1} = \mathbf{A} (\mathbf{D}_{\Omega\theta} [\vec{\lambda} \alpha_k - \Delta \vec{\theta}_{SE}] + \mathbf{D}_{\Omega\Omega} [\vec{\Omega}_k + \Gamma_a \vec{P}]) \quad (39)$$

Notice that the reference point in the cycle remains immediately after support transfer but *before* impulse application.

14 Steady walking conditions with pulsing

New steady walking conditions follow from exactly the same derivation as led to (21). With \vec{P} included, the steady-cycle $\vec{\Omega}$ (*cf.* (19)) is

$$\vec{\Omega}_0 = [\mathbf{I} - \Lambda \mathbf{D}_{\Omega\Omega}]^{-1} \Lambda [\mathbf{D}_{\Omega\theta} [\vec{\lambda}\alpha_0 - \Delta\vec{\theta}_{SE}] + \mathbf{D}_{\Omega\Omega} \Gamma_a \vec{P}_0] \quad (40)$$

The steady cycle conditions (*cf.* (21)) become

$$\vec{0} = [\mathbf{D}' - \mathbf{F}] \vec{\lambda}\alpha_0 - [\mathbf{D}' - \mathbf{I}] [\Delta\vec{\theta}_W + \vec{b}\gamma] + \mathbf{D}_{\theta\Omega} [\mathbf{I} - \Lambda \mathbf{D}_{\Omega\Omega}]^{-1} \Gamma_a \vec{P}_0 \quad (41)$$

If $\vec{P}_0 = 0$, this reduces to the condition for passive walking. A particularly attractive feature of impulse power is that the passive walking solution can be made independent of the slope. That is, \vec{P}_0 can be chosen to cancel the γ term in (41):

$$\vec{P}_0 = [\mathbf{D}_{\theta\Omega} [\mathbf{I} - \Lambda \mathbf{D}_{\Omega\Omega}]^{-1} \Gamma_a]^{-1} [\mathbf{D}' - \mathbf{I}] \vec{b} (\gamma - \gamma_P) \quad (42)$$

Then the same (α_0, τ_0) which satisfy (21) with $\vec{P}_0 = 0$ will continue to apply for all slopes. ($\vec{\Omega}$, however, will change with slope according to (40).) Thus while (42) is certainly not the only nor necessarily even the best choice for \vec{P}_0 , it does avoid the problems due to varying τ_0 which arise when one supplies energy by length variation or torque application. Moreover, another nice feature of (42) is that the direction of \vec{P}_0 is independent of γ .

15 Linearised step-to-step equations with pulsing

As always, once the steady cycle is found, its stability must be assessed by linearising the S-to-S equations. In this case,

$$\begin{bmatrix} \Delta\alpha_{k+1} \\ \Delta\vec{\Omega}_{k+1} \\ \Delta\tau_k \end{bmatrix} = \mathbf{S} \begin{bmatrix} \Delta\alpha_k \\ \Delta\vec{\Omega}_k \end{bmatrix} + \vec{h}\Delta\gamma + \mathbf{L}\Delta\vec{P} \quad (43)$$

If \vec{P} is invariant from step to step, then one can assess stability just by calculating the eigenvalues of \mathbf{S} . With example parameters as used for torque and length variation (figures 9 and 13), we found that constant- \vec{P} stability is not bad, but on the other hand not so good as one would like. At this point a happy coincidence emerges between what is practical to design, and what is desirable dynamically. Our plan is to apply the impulse by spring-driven pistons built into each leg. Each spring will be wound to a specified compression during the stance phase and triggered at support transfer. Two effects will then cause \vec{P} to *vary* with perturbations in the walking cycle. First, the angle

of application will vary with $\Delta\alpha$. This effect turns out to be somewhat destabilising. Second, the magnitude of \vec{P} will vary such that the *energy* delivered remains constant. Thus according to (32), if the leg speeds increase, the impulse decreases. This effect is strongly stabilising.

For our purposes, then, the most convenient control variables are not the two components of \vec{P} , but rather the energy input E and the angle of actuation relative to the leg ϵ . Appendix F shows how the linearised S-to-S equations (43) can be recast in terms of these variables; the result is

$$\begin{bmatrix} \Delta\alpha_{k+1} \\ \Delta\vec{\Omega}_{k+1} \\ \Delta\tau_k \end{bmatrix} = \mathbf{S}_e \begin{bmatrix} \Delta\alpha_k \\ \Delta\vec{\Omega}_k \end{bmatrix} + \vec{h}_e \Delta\gamma + \mathbf{B} \begin{bmatrix} \Delta E \\ \Delta\epsilon \end{bmatrix} \quad (44)$$

16 Stability of impulse-powered walking

Figure 15 shows the stability obtained with constant-energy pulsing of our example bipeds. \vec{P}_0 is chosen according to (42), and the impulse is applied at the foot's centre of curvature. This reason for choosing the centre of curvature is that the lower leg could be rotated about it (thus changing ϵ) without affecting other design parameters. As the figure shows, the choice has dynamical as well as mechanical appeal: stability is quite good over a broad range of uphill grades.

Up to this point we have limited attention to $\alpha_0 = 0.3$, which is representative of a "comfortable" gait. But both longer and shorter strides are also useful. Thus figure 16 provides examples of varying both α_0 and γ . (Note that only "uphill" slopes are plotted in this figure, *i.e.* with $P_x > 0$.) As the grade steepens the short-stride gaits break down first. Actually a static analysis suggests this result. Imagine the legs standing still with hip angle $2\alpha_0$, as in figure 7: the *static* stability of this stance becomes marginal as γ approaches $\pm\alpha_0$.

The actuator angles ϵ , as given by (42) for each value of α_0 , are tabulated in the figure. Since all ϵ values are quite small, it would seem sensible just to build the actuator parallel to the leg, *i.e.* $\epsilon = 0$. This option is explored in figure 17. It shows a significant reduction in the range of stable α_0 and γ , so walking is rather sensitive to ϵ . Indeed the margin for error in ϵ , even on a modest grade, is only of order 10mrad . Such high sensitivity raises concerns about the validity of the impulsive approximation. While the leg will not rotate very far in the finite time actually required to apply the impulse, the rotation will certainly be of order 10mrad or larger. Hence (42) may not estimate ϵ with sufficient accuracy for design. Instead appropriate settings might best be found by experimentation and, perhaps, closed-loop adjustment.

17 Stepping stone control by toe-off pulsing

Of course toe-off pulsing can be varied dynamically for step-to-step control. (38) can be used to formulate a control law, as in (29). The difficulty is that shortening of the step can easily call for the trailing foot to *pull* on the ground! Thus dynamic \vec{P} adjustment has its limitations, and must be supplemented by another control.

18 Walking with a perfectly stabilised torso

Since toe-off pulsing is good for uphill walking (figure 16), and stance torque for downhill walking (figure 9) these two methods are nicely complementary. But of course one needs some physical mechanism for applying stance torque. Leaning of the torso is the natural method. That is, holding the torso at some angle to the vertical calls for some steady torque; this can be supplied by reaction against the stance leg.

We have two methods for treating the torso analytically. The simpler involves specifying that the torso angle remains constant throughout the step. This cannot be precisely true, since an impulsive stance/torso torque would be required at support transfer. However, it seems a reasonable approximation for most practical walking systems, and it simplifies analysis. The more elaborate method allows the torso to sway, which adds two degrees of freedom (θ_T and Ω_T) to the stance and S-to-S dynamics. It also requires specification of a control law for torso angle. Fortunately, the constant- θ_T method provides a reasonably complete description of the role of the torso in walking; the swaying- θ_T method is mainly useful as a check on accuracy.

For the moment, then, suppose that the torso link is put on the legs as in figure 7, and that its angle can be held constant throughout the step. Two items must be added to the list of design parameters: the angle θ_T , and the torso mass centre, c_T . Stance, support transfer, impulse coupling, S-to-S, and steady walking equations can be derived by the same procedure as was followed above. In fact, the results are in form *exactly* the same as (36), (37), (13), (14), (35), (38), (39), (40), and (41). Only the definitions of terms change; these are presented in appendices A and C. The linearised S-to-S equations are also as in (44).

Now consider the variety of steady gaits possible for a given slope and stride length. In fully passive walking, γ determines α_0 and τ_0 uniquely. With \vec{P} as the control variable, one can choose all three independently. Here one can choose all three, *plus* θ_T . This freedom can be made explicit in the steady-cycle equations (41) by expressing $\Delta\vec{\theta}_{SE}$ as follows: (cf. (6))

$$\Delta\vec{\theta}_{SE} = \Delta\vec{\theta}_W + \vec{b}\gamma + \vec{a}_T\theta_T \quad (45)$$

Then the steady-cycle condition (41) becomes

$$\vec{0} = [\mathbf{D}' - \mathbf{F}] \vec{\lambda}\alpha_0 - [\mathbf{D}' - \mathbf{I}] [\Delta\vec{\theta}_W + \vec{b}\gamma + \vec{a}_T\theta_T] + \mathbf{D}_{\theta\Omega}[\mathbf{I} - \Lambda\mathbf{D}_{\Omega\Omega}]^{-1}\Gamma_a\vec{P}_0 \quad (46)$$

While θ_T can be chosen freely, it seems natural to vary it with γ so that the torso attitude is constant with respect to the vertical. An appropriate choice for \vec{P}_0 , analogous to (42), is then

$$\vec{P}_0 = [\mathbf{D}_{\theta\Omega}[\mathbf{I} - \Lambda\mathbf{D}_{\Omega\Omega}]^{-1}\Gamma_a]^{-1} [\mathbf{D}' - \mathbf{I}](\vec{b} + \vec{a}_T)(\gamma - \gamma_P) \quad (47)$$

This condition is not obligatory, but it does have the attractive feature, in common with (42), of making both τ_0 and ϵ invariant with γ .

Figure 18 illustrates solutions for (46) over a range of both up- and downhill slopes. Essentially the plot gives the control to use for steady walking at any selected α_0 and γ . The parameters are similar to those in previous examples, except that we have added $c_T = 0.3$. Starting at the right (downhill) end of the plot, $\vec{P} = 0$ and the gait is established by leaning the torso backward. As the slope moderates, so does the torso's recline, eventually reaching $\theta_T = -\gamma$, *i.e.* vertical. From that point $\theta_T = -\gamma$ is maintained, and \vec{P}_0 is selected according to (47).

Figure 19 indicates the corresponding step period and stability for striding with $\alpha_0 = 0.3$. In this example stable walking can be established by torso inclination alone on downhill grades ranging from zero to slightly more than 10%. Torso-controlled uphill walking is precluded by an unacceptably short step period, as in figure 9. So for uphill walking, $\theta_T + \gamma$ can be fixed, and \vec{P} selected according to (47). However, (47) applies only over the range of torso angles for which there exist "downhill" walking solutions. If one wants to lean further forward, or change the step period from that used in downhill walking, then one can return to the steady-cycle condition (46) and calculate the appropriate \vec{P}_0 . This strategy is perfectly satisfactory, although it does carry the cost of varying ϵ with slope. Also, it fails if the slope calls for the trailing foot to pull rather than push; hence the gap between the "uphill" and "downhill" solutions. An alternative is to shift the range of θ_T for "downhill" walking by adjusting w , as shown in figure 22. The penalty in that strategy (as demonstrated by γ vs w in figure 10) is slightly higher specific resistance.

Thus addition of a torso creates quite a variety of walking solutions, but they can all be understood in terms of legs-only walking. Actually figure 19 is little more than a composite of results for stance torquing (figure 9) and toe-off pulsing (figure 15). So the overall message of figures 18 and 19 bears out the qualitative concept of the torso's role in walking: it can be used to generate stance torque, while leaving the walking mode intact.

19 Stance dynamics with a swaying torso

So far so good, but figures 18 and 19 were calculated with the torso perfectly stabilised. In practice, of course, it is jerked forward at support transfer. Presumably if the return is

rapid, then the gait will be very close to that calculated with perfect torso stabilisation. But in any case a precise calculation is quite straightforward.

Actually the analysis remains in form very much the same as always. But an important new term is *active* control to keep the torso upright. An appropriate control law can be formulated most easily if one imagines planting the legs firmly on the ground. Then the torso becomes an ordinary inverted pendulum, with (dimensionless) equation of motion

$$m_T (c_T^2 + r_{gyr_T}^2) \ddot{\theta}_T \approx m_T c_T (\theta_T + \gamma) + T_{CT} \quad (48)$$

One has a great deal of freedom in choosing the control torque T_{CT} , but for our purposes simple linear feedback is quite satisfactory:

$$T_{CT} = k_T(\theta_T^* - \theta_T - \tau_T \Omega_T) \quad (49)$$

The closed-loop natural frequency is then

$$\omega_T = \sqrt{\frac{k_T - m_T c_T}{m_T (c_T^2 + r_{gyr_T}^2)}} \quad (50)$$

The damping ratio is

$$\zeta_T = \frac{k_T \tau_T}{2 \omega_T} m_T (c_T^2 + r_{gyr_T}^2) \quad (51)$$

Steady-state angle and torque are

$$\theta_{TSS} = \theta_T^* + \left(\frac{c_T}{\omega_T^2 (c_T^2 + r_{gyr_T}^2)} \right) (\theta_T^* + \gamma) \quad (52)$$

$$T_{CTSS} = k_T(\theta_T^* - \theta_{TSS}) \quad (53)$$

With $\omega_T \gg 1/\tau_0$, and $\zeta_T \approx 1$, θ_T is held nearly constant at θ_T^* - *i.e.* the perfectly stabilised case. At issue here is how smaller ω_T affects the walk. Notice that torso sway brings three new parameters into the model: ω_T , ζ_T , and r_{gyr_T} .

For analysis of swaying-torso walking, the stance equations are a 3×3 version of (4) with terms modified as discussed in appendix A. Note that $\vec{\theta}$ is now

$$\vec{\theta} \equiv \begin{bmatrix} \theta_C \\ \theta_F \\ \theta_T \end{bmatrix} \quad (54)$$

The torque vector has the gravitational component as in (5), plus the active control:

$$\vec{T} = \mathbf{K}_T[\Delta\vec{\theta}_{SET} - \Delta\vec{\theta}] + \begin{bmatrix} -T_{CT} \\ 0 \\ T_{CT} \end{bmatrix} \quad (55)$$

Note that T_{CT} is supplied by a reaction against the stance leg, while the swing leg is left free. (At support transfer the torso actuator must switch legs promptly; otherwise the erstwhile stance leg, having suddenly become much easier to move, would be launched on an errant trajectory.) Inserting the torso control law (49) and collecting terms leaves the stance equations in the form

$$\mathbf{M}_{T0}\dot{\vec{\Omega}} + \mathbf{C}_T\vec{\Omega} + \mathbf{K}_T^*\Delta\vec{\theta} = \mathbf{K}_T^*\Delta\vec{\theta}_{SET}^* \quad (56)$$

The damping matrix is

$$\mathbf{C}_T = \begin{bmatrix} 0 & 0 & -k_T & \tau_T \\ 0 & 0 & 0 & 0 \\ 0 & 0 & k_T & \tau_T \end{bmatrix} \quad (57)$$

The modified stiffness matrix is

$$\mathbf{K}_T^* = \mathbf{K}_T + \begin{bmatrix} 0 & 0 & -k_T \\ 0 & 0 & 0 \\ 0 & 0 & k_T \end{bmatrix} \quad (58)$$

The new static equilibrium is

$$\Delta\vec{\theta}_{SET}^* = \mathbf{K}_T^{*-1} \left(\mathbf{K}_T\Delta\vec{\theta}_{SET} + \begin{bmatrix} -k_T \theta_T^* \\ 0 \\ k_T \theta_T^* \end{bmatrix} \right) \quad (59)$$

or, by analogy with (6)

$$\Delta\vec{\theta}_{SET}^* = \Delta\vec{\theta}_{WT}^* + \vec{b}_T^* \gamma + \vec{a}_T \theta_T^* \quad (60)$$

The solution of the stance equations (56) has the same form as (7), (8), but with $\vec{\theta}$ and $\vec{\Omega}$ redefined, $\Delta\vec{\theta}_{SET}^*$ substituted for $\Delta\vec{\theta}_{SE}$, and 3×3 transition matrices.

20 Support transfer and impulse coupling with a swaying torso

The step starts when the leg angles satisfy (9), *i.e.* equal and opposite if the leg lengths are equal. However, the torso angle can be specified independently, so

$$\Delta\vec{\theta}_k \equiv \begin{bmatrix} \vec{\lambda}\alpha_k \\ \Delta\theta_{T_k} \end{bmatrix} \quad (61)$$

In support transfer the leg indices are flipped, while the torso angle remains constant. Thus the flip matrix (12) must be redefined as

$$\mathbf{F} \equiv \begin{bmatrix} 0 & 1 & 0 \\ 1 & 0 & 0 \\ 0 & 0 & 1 \end{bmatrix} \quad (62)$$

Then

$$\Delta \vec{\theta}_{k+1} = \mathbf{F} \Delta \vec{\theta}(\tau_k) \quad (63)$$

Meanwhile the speed change is calculated just as in (14), with Λ_T now 3×3 . Λ_T is derived in appendix C. Impulse coupling immediately after support transfer is also calculated just as in (35), with M_T now 3×3 , and G_a 2×3 .

21 Nonlinear step-to-step equations with a swaying torso

Redefinition of $\Delta \vec{\theta}$ at support transfer (61) calls for a minor change in notation for the S-to-S equations (38), (39). $\vec{\lambda}\alpha_k$ is replaced in favour of $\Delta \vec{\theta}_k$; thus

$$\Delta \vec{\theta}_{k+1} = \mathbf{F} \left(\mathbf{D}_{\theta\theta} [\Delta \vec{\theta}_k - \Delta \vec{\theta}_{SET}^*] + \mathbf{D}_{\theta\Omega} [\vec{\Omega}_k + \Gamma_a \vec{P}] + \Delta \vec{\theta}_{SET}^* \right) \quad (64)$$

$$\vec{\Omega}_{k+1} = \Lambda_T \left(\mathbf{D}_{\Omega\theta} [\Delta \vec{\theta}_k - \Delta \vec{\theta}_{SET}^*] + \mathbf{D}_{\Omega\Omega} [\vec{\Omega}_k + \Gamma_a \vec{P}] \right) \quad (65)$$

22 Steady walking with a swaying torso

The steady walking conditions also involve a small change in notation. From (40), (41), these become

$$\vec{\Omega}_0 = [\mathbf{I} - \Lambda_T \mathbf{D}_{\Omega\Omega}]^{-1} \Lambda_T \left[\mathbf{D}_{\Omega\theta} [\Delta \vec{\theta}_0 - \Delta \vec{\theta}_{SET}^*] + \mathbf{D}_{\Omega\Omega} \Gamma_a \vec{P}_0 \right] \quad (66)$$

$$\vec{0} = [\mathbf{D}' - \mathbf{F}] \Delta \vec{\theta}_0 - [\mathbf{D}' - \mathbf{I}] [\Delta \vec{\theta}_{WT}^* + \vec{b}_T^* \gamma + \vec{a}_T \theta_T^*] + \mathbf{D}_{\theta\Omega} [\mathbf{I} - \Lambda_T \mathbf{D}_{\Omega\Omega}]^{-1} \Gamma_a \vec{P}_0 \quad (67)$$

One can use this last formula in a variety of ways. As in the solution for passive walking, one can specify $\Delta \vec{\theta}_0$ - *i.e.* the stride length, and torso angle at the start-of-step - and solve for τ_0 , γ , and θ_T^* . Alternatively, one can specify $\Delta \vec{\theta}_0$, τ_0 , and γ , and solve for \vec{P}_0 and θ_T^* .

23 Linearised step-to-step equations with a swaying torso

The linearised S-to-S equations become fifth order, with θ_T and Ω_T added to the state vector. Derivation proceeds as for (44), with the original gradients modified, and new terms added for θ_T , Ω_T , and θ_T^* . The result is

$$\begin{bmatrix} \Delta\alpha_{k+1} \\ \Delta\theta_{T_{k+1}} \\ \Delta\vec{\Omega}_{k+1} \\ \Delta\tau_k \end{bmatrix} = \mathbf{S}_e \begin{bmatrix} \Delta\alpha_k \\ \Delta\theta_{T_k} \\ \Delta\vec{\Omega}_k \end{bmatrix} + \vec{h}_e \Delta\gamma + \vec{a}' \Delta\theta_T^* + \mathbf{B} \begin{bmatrix} \Delta E \\ \Delta\epsilon \end{bmatrix} \quad (68)$$

24 Examples of walking with a swaying torso

Now consider a few examples. First, figure 20 shows a walking cycle including a swaying torso. Torso stabilisation is rather soft in this case, so that the jerk at support transfer is followed by a pronounced forward sway and recovery requiring the full step period. Since the torso has $\theta_T > 0$ throughout the cycle, the average stance torque is positive, and this reduces the step period just as in figure 9 – with the same unhappy consequences for the walking cycle. This is shown by figure 21: as torso stabilisation softens, the step period decreases and ultimately disappears. As ever, the remedy is a negative shift in w , which allows walking with quite slow control at the cost of slightly higher specific resistance. So the message is that torso sway is tolerable but certainly not desirable.

Figure 22 takes up the question of slope. In this case we have included an example of using w to shift the range of “downhill” walking. Otherwise the same variety of solutions appears as in figure 19, and the same explanations apply. So while swaying-torso calculations are much more elaborate than steady-torso, or indeed legs-only calculations, the results are much the same – which, of course, is the simplest and best of all possible outcomes.

25 Step-to-step gait variation with a swaying torso

Earlier we discussed “stepping stone” control for a legs-only biped by step-to-step adjustment of stance and hip torque. At the time we didn’t specify how the stance torque might be applied. Now it is clear that torquing against the torso is effective for *steady* walking, and so one wonders whether it is equally effective for step-to-step adjustments.

In this case, unfortunately, dynamics conspire against us. Imagine making a move that calls for positive stance torque. To generate the torque in steady walking, one rotates the torso forward. But dynamically, when the torso moves forward, the hip

recoils backward; thus the immediate effect on the stance leg is roughly opposite to that intended! The consequences emerge if one attempts to formulate a stepping-stone controller analogous to (29). That is, solve the (θ_C, θ_F) S-to-S equations (64) for the control inputs $(\Delta\theta_T^*, \Delta T_H)$ required to take a step of the desired length α_{k+1} and period τ_k . (The swaying-torso rather than steady-torso equations must be used, since only the swaying-torso equations account for the recoil produced by a dynamic change in θ_T .) If one puts the resulting control law back into the S-to-S equations, one finds that α_{k+1} and τ_k are regulated exactly as intended, but the remaining state variables go unstable! The physical problem is that the controller has to use the recoil to get the immediately desired result, but then is left with an untenable “static” torque.

The instability might be ameliorated by a different control law, but the fundamental problem is that torso leaning isn’t physically appropriate for dynamic gait control. Fortunately there are several alternatives. For example, torque adjustments might be made by a momentum wheel in the torso. (Accumulated momentum would then be dumped slowly, against a gravitational torque.) Or stance torque could be dropped entirely as a dynamic control, and leg length or w used instead. We are now exploring the options to find the best dynamical and mechanical strategy. So further analysis of stepping-stone control is left for a later paper, and we can now bring this report to a close.

26 Summary

Figure 20 shows the walking cycle with a swaying torso, and is accompanied by a rather formidable list of parameters which reflects the large number of terms affecting the motion. When faced with an elaborate model producing lengthy equations such as (67), there is some danger that the essential effects will not be easily recognised. But we hope that by starting the discussion with simpler bipeds and working to the more complex we have conveyed the simple dynamics of walking which is common across a wide range of parameter variations and control techniques. To make the point, compare figures 6 and 20. The former, showing the walking cycle of a synthetic wheel, involves nothing more complicated than a simple pendulum. Its cycle is easily understood; a key result is that the step period satisfies $\omega_F\tau_0 = 4.058$. By comparison the swaying torso example, with swing mode frequency $\omega_F = 1.30$, has $\omega_F\tau_0 = 3.86$; this differs from the synthetic wheel value by only 5%. So if one understands completely walking by a synthetic wheel, then one understands 95% of walking by an apparently much more complicated system!

Thus all of our elaborate analysis has not introduced any new physics, but rather has simply accounted for a few numerical details, and more importantly defined the range of conditions over which common behaviour applies. The news is good. To draw another analogy, aircraft have their characteristic ways of oscillating, with the same set of modes common among designs ranging from sailplanes to airliners to Space Shuttles. Ships also have their characteristic dynamics, as do horns, and so on. Our point is

that a pair of coupled pendula also has its natural modes, and one of them is walking. The walking mode is not quite so robust as, say, the phugoid mode among aircraft, but nevertheless it is present and moreover stable across a wide range of design variations. Furthermore, just as one can play a tune on a horn, so one can learn to pump energy into the walking mode, to tune it and modulate it, in order to move with dexterity and flexibility. Of course use of the walking mode is not obligatory; actuators could be installed to make the legs move in any way one chose. However, using an unnatural gait is roughly analogous to forcing a horn away from resonance. Better to concentrate on where you want to go, and let nature work out the details.

APPENDICES

A Stance dynamics with swaying torso

We now derive the linearised equations of motion for the stance phase, including torso sway. The legs-only and fixed-torso equations (4) emerge as special cases. Refer to the 2-D biped as sketched in figure 7. For consistency with [McGeer 88], and following the convention for a multi-link kinematic chain, we say that with both legs parallel to the surface normal $\theta_C = 0$ and $\theta_F = \pi$. By the same convention, w is positive-forward for the stance leg, and positive-aft for the swing leg. Thus on support transfer the leg angles switch by π , and w changes sign.

For the swing leg and torso, the equations of motion are

$$\frac{dH}{dt} = T \tag{69}$$

where T is the torque on the element, and H is its angular momentum about the hip. For the stance leg a similar equation holds, with H the total angular momentum of all elements and T the total torque about the point of contact. However, it is easiest to subtract the swing leg and torso equations from the stance leg equation; then

$$\frac{d}{dt}(H_C - H_F - H_T) = T_{total} - T_F - T_T \equiv T_C \tag{70}$$

T_C is the torque acting *directly* on the stance leg about the point of contact.

The angular momentum of the swing leg is

$$H_F = m_F(r_{gyr_F}^2 \Omega_F + \vec{r}_{HF} \times \vec{V}_F) \tag{71}$$

where \vec{r}_{HF} is the vector from the hip to the swing leg's mass centre. \vec{V}_F is the velocity of its mass centre. The expression for the torso is the same except subscript T replaces

F. For the stance leg,

$$H_C - H_F - H_T = m_C(r_{gyr_C}^2 \Omega_C + \vec{r}_{CC} \times \vec{V}_C) + \vec{r}_{CH} \times (m_F \vec{V}_F + m_T \vec{V}_T) \quad (72)$$

Here \vec{r}_{CC} is the vector from contact point to stance leg *c.m.*, and \vec{r}_{CH} from contact point to hip. The velocity vectors in turn are

$$\vec{V}_C = \Omega_C \times \vec{r}_{CC} \quad (73)$$

$$\vec{V}_F = \Omega_C \times \vec{r}_{CH} + \Omega_F \times \vec{r}_{HF} \quad (74)$$

and similarly for \vec{V}_T . Substituting back into (71) and (72), and working out the vector products, leaves a matrix formula for the angular momenta. Define

$$I_C \equiv m_C \left(r_{gyr_C}^2 + c_C^2 + w_C^2 + 2R(c_C - R)(\cos \theta_C - 1) \right) - \frac{2m_C R w_C \sin \theta_C}{(m_F + m_T)(l_C^2 + 2R^2 - 2l_C R + 2R(l_C - R) \cos \theta_C)} \quad (75)$$

$$I_F \equiv m_F \left(r_{gyr_F}^2 + (l_F - c_F)^2 + w_F^2 \right) \quad (76)$$

$$I_{FC} \equiv m_F(l_C - R) \left((l_F - c_F) \cos(\theta_F - \theta_C) - w_F \sin(\theta_F - \theta_C) \right) + m_F R \left((l_F - c_F) \cos \theta_F - w_F \sin \theta_F \right) \quad (77)$$

and similarly for the torso, replacing subscript *F* by *T*, $(l_F - c_F)$ by c_T , and $w = 0$. Then the angular momentum vector is

$$\vec{H} = \begin{bmatrix} H_C - H_F - H_T \\ H_F \\ H_T \end{bmatrix} = \begin{bmatrix} I_C & I_{FC} & I_{TC} \\ I_{FC} & I_F & 0 \\ I_{TC} & 0 & I_T \end{bmatrix} \begin{bmatrix} \Omega_C \\ \Omega_F \\ \Omega_T \end{bmatrix} \equiv \mathbf{M}_T \vec{\Omega} \quad (78)$$

Differentiating formulates the LHS of the equations of motion (69), (70), which has one term in $d\vec{\Omega}/dt$, and another in $\vec{\Omega}^2$. In walking the latter (centrifugal) term is negligible, so for our purposes

$$\frac{d\vec{H}}{dt} \approx \mathbf{M}_{T0} \frac{d\vec{\Omega}}{dt} \quad (79)$$

\mathbf{M}_{T0} is the inertia matrix \mathbf{M}_T evaluated in the reference state for linearisation, namely $\theta_C = \theta_T = 0$, $\theta_F = \pi$.

Now to work on the torque terms in the equations of motion. The principle torque is due to gravity:

$$\vec{T}_{gF} = m_F \vec{r}_{HF} \times \vec{g}$$

$$= m_F g ((l_F - c_F) \sin(\theta_F + \gamma) + w_F \cos(\theta_F + \gamma)) \quad (80)$$

$$\begin{aligned} \vec{T}_{gC} &= T_{gtotal} - \vec{T}_{gF} - \vec{T}_{gT} \\ &= m_C \vec{r}_{CC} \times \vec{g} + (m_F + m_T) \vec{r}_{CH} \times \vec{g} \\ &= mgR \sin \gamma + g m_C w_C \cos(\theta_C + \gamma) + \\ &\quad g (m_C(c_C - R) + (m_F + m_T)(l_C - R)) \sin(\theta_C + \gamma) \end{aligned} \quad (81)$$

Linearising about the reference state, and for small γ , leaves

$$\vec{T}_{gF} \approx -m_F g ((l_F - c_F)(\Delta\theta_F + \gamma) + w_F) \quad (82)$$

and similarly for the torso, except that $(l_F - c_F)$ becomes c_T , and $w = 0$. For the stance leg,

$$\begin{aligned} \vec{T}_{gC} \approx & g (m_C (c_C - R) + (m_F + m_T)(l_C - R)) \Delta\theta_C + \\ & g (m_C c_C + (m_F + m_T) l_C) \gamma + g m_C w_C \end{aligned} \quad (83)$$

To express the gravitational torque in matrix form, define

$$\mathbf{K}_T \equiv g \begin{bmatrix} m_C (c_C - R) + & 0 & 0 \\ (m_F + m_T)(l_C - R) & & \\ 0 & -m_F (l_F - c_F) & 0 \\ 0 & 0 & m_T c_T \end{bmatrix} \quad (84)$$

$$\Delta\vec{\theta}_{WT} \equiv -g\mathbf{K}_T^{-1} \begin{bmatrix} m_C w_C \\ -m_F w_F \\ 0 \end{bmatrix} \quad (85)$$

$$\vec{b}_T \equiv -g\mathbf{K}_T^{-1} \begin{bmatrix} m_C c_C + (m_F + m_T) l_C \\ -m_F (l_F - c_F) \\ m_T c_T \end{bmatrix} \quad (86)$$

Substituting these and the angular momentum terms (79) into the equations of motion (69), (70) produces

$$\mathbf{M}_{T0} \dot{\vec{\Omega}} + \mathbf{K}_T \Delta\vec{\theta} = \mathbf{K}_T [\Delta\vec{\theta}_{WT} + \vec{b}_T \gamma] + \Delta\vec{T} \quad (87)$$

B Stance dynamics with perfectly stabilised torso

The torso angle can be held constant during the step by applying a torque at the hip such that (87) is satisfied with $\Omega_T = 0$. Thus solving the third (torso) equation in (87) for the required torque (using (78)) gives

$$T_{CT} = I_{TC} \frac{d\Omega_C}{dt} - m_T c_T g (\Delta\theta_T + \gamma) \quad (88)$$

We specify that the reaction torque acts on the stance leg. Thus adding $-T_{CT}$ to the first equation in (87) modifies the inertia matrix \mathbf{M}_T and the static equilibrium vector. The new inertia matrix, from (78), is

$$\mathbf{M} = \begin{bmatrix} I_C + I_{TC} & I_{FC} \\ I_{FC} & I_F \end{bmatrix} \quad (89)$$

The static equilibrium is as expressed in (45), with

$$\vec{b}_T \equiv -g\mathbf{K}^{-1} \begin{bmatrix} m_C c_C + m_F l_C + m_T (l_C + c_T) \\ -m_F (l_F - c_F) \end{bmatrix} \quad (90)$$

$$\vec{a}_T = -g\mathbf{K}^{-1} \begin{bmatrix} m_T c_T \\ 0 \end{bmatrix} \quad (91)$$

\mathbf{K} is the upper 2×2 submatrix of \mathbf{K}_T , and $\Delta\vec{\theta}_W$ the upper 2 elements of $\Delta\vec{\theta}_{WT}$. The linearised stance equations are then as given in (4).

C Support transfer with swaying torso

In support transfer conservation holds for angular momenta of trailing leg and torso about the hip, and of the whole system about the *post*-transfer support point. Post-transfer, the angular momentum is as given by (78). Note that this involves the *exact* inertia matrix \mathbf{M}_T^+ evaluated for $\vec{\theta}$ at the instant of support transfer (as opposed to the legs-vertical matrix \mathbf{M}_{T0}). Before transfer a similar expression applies, but the inertia matrix (\mathbf{M}_T^-) is different since the system is rotating about the trailing rather than leading leg. To formulate \mathbf{M}_T^- one follows the same derivation as for \mathbf{M}_T^+ , using the post-transfer expressions for angular momenta (71), (72), but the *pre*-transfer expressions for velocities. Also one must be careful to index the legs properly: at support transfer swing and stance legs exchange roles, the angle of each rotates by π , and w changes sign. In the end, \mathbf{M}_T^- is as follows. Define

$$I_C^- = m_C \left(r_{gyr_C}^2 + w_C^2 - (l_C - c_C) ((c_C - R) + R \cos \theta_C) - R w_C \sin \theta_C \right) \quad (92)$$

$$\begin{aligned} I_{FC}^- &= m_C (R - l_F) ((c_C - R) \cos(\theta_C - \theta_F) - w_C \sin(\theta_C - \theta_F)) + \\ & m_C R ((c_C - R) \cos \theta_C - w_C \sin \theta_C + R + (R - l_F) \cos \theta_F) + \\ & m_F (l_C - R) ((R - c_F) \cos(\theta_C - \theta_F) + w_F \sin(\theta_C - \theta_F)) + \\ & m_F R ((R - c_F) \cos \theta_F - w_F \sin \theta_F + R + (l_C - R) \cos \theta_C) + \end{aligned}$$

$$m_T(l_C - R)((R - l_F) \cos(\theta_C - \theta_F) + R \cos \theta_C) + m_T R(R + (R - l_F) \cos \theta_F) \quad (93)$$

$$I_{TC}^- = m_T c_T (R \cos \theta_T + (l_C - R) \cos(\theta_C - \theta_T)) \quad (94)$$

$$I_F^- = m_F (r_{gyr_T}^2 + (l_F - c_F)(R - c_F) + w_F^2) + m_F R((l_F - c_F) \cos \theta_F - w_F \sin \theta_F) \quad (95)$$

$$I_{TF}^- = m_T c_T (R \cos \theta_T - (l_F - R) \cos(\theta_T - \theta_F)) \quad (96)$$

Then

$$\mathbf{M}_T^- = \begin{bmatrix} I_C^- & I_{FC}^- & I_{TC}^- \\ 0 & I_F^- & 0 \\ 0 & I_{TF}^- & I_T^- \end{bmatrix} \quad (97)$$

Thus conservation of angular momenta requires that

$$\mathbf{M}_T^+ \vec{\Omega}^+ = \mathbf{M}_T^- \vec{\Omega}^- \quad (98)$$

where $\vec{\Omega}^-$ is ordered according to the post-transfer indexing, *i.e.* leading leg, trailing leg, torso:

$$\vec{\Omega}^- = \mathbf{F} \vec{\Omega}(\tau_k) \quad (99)$$

Thus solving (98) for $\vec{\Omega}^+$ produces the swaying-torso analog of (14), with

$$\Lambda_T \equiv \mathbf{M}_T^{+1} \mathbf{M}_T^- \mathbf{F} \quad (100)$$

D Support transfer with perfectly stabilised torso

Normally the torso would be jerked forward in support transfer. However, forward rotation could be prevented by applying a rotational impulse \mathcal{H} between the torso and the post-transfer stance leg. Thus (98) becomes

$$\mathbf{M}_T^+ \vec{\Omega}^+ = \mathbf{M}_T^- \vec{\Omega}^- + \begin{bmatrix} -\mathcal{H} \\ 0 \\ \mathcal{H} \end{bmatrix} \quad (101)$$

One solves the third (torso) equation of this set for \mathcal{H} such that $\Omega_T^+ = \Omega_T^- = 0$, and puts $-\mathcal{H}$ into the first equation. This modifies the mass matrices just as in the equations of motion. One obtains a 2×2 system,

$$\mathbf{M}^+ \vec{\Omega}^+ = \mathbf{M}^- \vec{\Omega}^- \quad (102)$$

\mathbf{M}^+ is as given in (89), and from (98)

$$\mathbf{M}^- = \begin{bmatrix} I_C^- & I_{FC}^- + I_{TF}^- \\ 0 & I_F^- \end{bmatrix} \quad (103)$$

E Linearisation of the step-to-step equations

Linearisation of the S-to-S equations (38), (39) or (64), (65) becomes a lengthy process if one tries to write out each matrix derivative in full detail. We will not go that far here, but rather only indicate which matrix derivatives appear.

Take the swaying-torso S-to-S equations (64), (65). (The fixed-torso and legs-only cases are similar.) Following (25), the function to be linearised – a vector of length 6 – is

$$\vec{f} = \left[\frac{\mathbf{F} \left(\mathbf{D}_{\theta\theta} [\Delta\vec{\theta}_k - \Delta\vec{\theta}_{SET}^*] + \mathbf{D}_{\theta\Omega} [\vec{\Omega}_k + \Gamma_a \vec{P}] + \Delta\vec{\theta}_{SET}^* \right) - \Delta\vec{\theta}_{k+1}}{\Lambda_T \left(\mathbf{D}_{\Omega\theta} [\Delta\vec{\theta}_k - \Delta\vec{\theta}_{SET}^*] + \mathbf{D}_{\Omega\Omega} [\vec{\Omega}_k + \Gamma_a \vec{P}] \right) - \vec{\Omega}_{k+1}} \right] \quad (104)$$

This is to be expanded in a Taylor series in several variables. It is essential to include at least 11 variables, namely α , θ_T , $\vec{\Omega}$ at the start of steps k and $k+1$, and τ_k . \vec{P} must be added to the list if it varies from step to step, and several more variables might be added for use in “stepping stone” control, *e.g.* l_C , l_F at the start of steps k and $k+1$; θ_T^* , T_C , T_H during step k , and perhaps γ although, as explained earlier, the S-to-S equations as derived are *not* valid for dynamic changes in slope. This list is by no means exclusive, but it includes the variables of present interest. The terms in \vec{f} affected by these variables are listed below.

ELEMENT	ESSENTIAL VARIABLES	DISCRETIONARY VARIABLES
$\Delta\vec{\theta}_{k+1}$	$\alpha_{k+1}, \theta_{T_{k+1}}$	$l_{C_{k+1}}, l_{F_{k+1}}$
$\vec{\Omega}_{k+1}$	$\vec{\Omega}_{k+1}$	-
$\Delta\vec{\theta}_k$	α_k, θ_{T_k}	l_{C_k}, l_{F_k}
$\vec{\Omega}_k$	$\vec{\Omega}_k$	-
$\Delta\vec{\theta}_{SET}^*$	-	$T_C, T_H, \theta_T^*, \gamma$
\vec{P}	-	\vec{P}
Γ_a	α_k, θ_{T_k}	l_{C_k}, l_{F_k}
Λ_T	α_k, θ_{T_k}	l_{C_k}, l_{F_k}
$D_{\theta\theta}, D_{\theta\Omega}, D_{\Omega\theta}, D_{\Omega\Omega}$	τ_k	-

The partials of \vec{f} with respect to the "essential" variables are then as follows:

$$\frac{\partial \vec{f}}{\partial \alpha_{k+1}} = - \left[\frac{\frac{\partial \Delta\vec{\theta}}{\partial \alpha}}{\vec{0}} \right] + \left[\frac{0}{\frac{\partial \Lambda_T}{\partial \alpha} [D_{\Omega\theta}[\Delta\vec{\theta}_0 - \Delta\vec{\theta}_{SET}^*] + D_{\Omega\Omega}[\vec{\Omega}_0 + \Gamma_a \vec{P}_0]]} \right] \quad (105)$$

and similarly for $\partial \vec{f} / \partial \theta_{T_{k+1}}$.

$$\frac{\partial \vec{f}}{\partial \Omega_{C_{k+1}}} = - \left[\frac{\vec{0}}{\frac{\partial \vec{\Omega}}{\partial \Omega_C}} \right] \quad (106)$$

and similarly for $\Omega_{F_{k+1}}, \Omega_{T_{k+1}}$.

$$\frac{\partial \vec{f}}{\partial \alpha_k} = \left[\frac{\mathbf{FD}_{\theta\theta}}{\Lambda_T \mathbf{D}_{\Omega\theta}} \right] \frac{\partial \Delta\vec{\theta}}{\partial \alpha} + \left[\frac{\mathbf{FD}_{\theta\Omega}}{\Lambda_T \mathbf{D}_{\Omega\Omega}} \right] \frac{\partial \Gamma_a \vec{P}_0}{\partial \alpha} \quad (107)$$

and similarly for θ_{T_k} .

$$\frac{\partial \vec{f}}{\partial \Omega_{C_k}} = \left[\frac{\mathbf{FD}_{\theta\Omega}}{\Lambda_T \mathbf{D}_{\Omega\Omega}} \right] \frac{\partial \vec{\Omega}}{\partial \Omega_C} \quad (108)$$

and similarly for Ω_{Fk}, Ω_{Tk} .

$$\frac{\partial \vec{f}}{\partial \tau_k} = \left[\begin{array}{c|c} \mathbf{F} \frac{\partial \mathbf{D}_{\theta\theta}}{\partial \tau} & \mathbf{F} \frac{\partial \mathbf{D}_{\theta\Omega}}{\partial \tau} \\ \hline \Lambda_{\mathbf{T}} \frac{\partial \mathbf{D}_{\Omega\theta}}{\partial \tau} & \Lambda_{\mathbf{T}} \frac{\partial \mathbf{D}_{\Omega\Omega}}{\partial \tau} \end{array} \right] \left[\begin{array}{c} [\Delta \vec{\theta}_0 - \Delta \vec{\theta}_{SET}^*] \\ \hline \vec{\Omega}_0 + \Gamma_a \vec{P}_0 \end{array} \right] \quad (109)$$

Also, if \vec{P} varies from step to step, then one needs

$$\frac{\partial \vec{f}}{\partial \vec{P}} = \left[\begin{array}{c} \mathbf{F} \mathbf{D}_{\theta\Omega} \\ \hline \Lambda_{\mathbf{T}} \mathbf{D}_{\Omega\Omega} \end{array} \right] \Gamma_a \mathbf{I} \quad (110)$$

A few notes are in order concerning these formulas. First, in (105) and (107), $\partial \Delta \vec{\theta} / \partial \alpha$ has contributions from both θ_C and θ_F :

$$\frac{\partial \Delta \vec{\theta}}{\partial \alpha} = \left[\begin{array}{c} -1 \\ \partial \theta_F / \partial \alpha \\ 0 \end{array} \right] \quad (111)$$

$\partial \theta_F / \partial \alpha$ follows from the support transfer condition (9).

In (105), $\partial \Lambda_{\mathbf{T}} / \partial \alpha$ is computed from the definition of $\Lambda_{\mathbf{T}}$ (100), as follows:

$$\frac{\partial \Lambda_{\mathbf{T}}}{\partial \alpha} = \frac{\partial \mathbf{M}_T^{+-1}}{\partial \alpha} \mathbf{M}_T^- \mathbf{F} + \mathbf{M}_T^{+-1} \frac{\partial \mathbf{M}_T^-}{\partial \alpha} \mathbf{F} \quad (112)$$

But

$$\frac{\partial \mathbf{M}_T^{+-1}}{\partial \alpha} = -\mathbf{M}_T^{+-1} \frac{\partial \mathbf{M}_T^+}{\partial \alpha} \mathbf{M}_T^{+-1} \quad (113)$$

So

$$\frac{\partial \Lambda_{\mathbf{T}}}{\partial \alpha} = \mathbf{M}_T^{+-1} \left[\frac{\partial \mathbf{M}_T^-}{\partial \alpha} \mathbf{F} - \frac{\partial \mathbf{M}_T^+}{\partial \alpha} \Lambda_{\mathbf{T}} \right] \quad (114)$$

The impulse-coupling matrix Γ_a also involves a term in \mathbf{M}_T^{-1} (35), so its derivative is computed in the same way.

In (109), the time derivative of the transition matrix \mathbf{D} is computed as follows. Excluding control torques, the stance equations (56) can be written in standard first-

order form as follows:

$$\begin{aligned} \frac{d}{dt} \begin{bmatrix} \Delta\vec{\theta} - \Delta\vec{\theta}_{SET}^* \\ \vec{\Omega} \end{bmatrix} &= \begin{bmatrix} \mathbf{0} & | & \mathbf{I} \\ \hline -\mathbf{M}_0^{-1}\mathbf{C}_T & | & -\mathbf{M}_0^{-1}\mathbf{K}_T^* \end{bmatrix} \begin{bmatrix} \Delta\vec{\theta} - \Delta\vec{\theta}_{SET}^* \\ \vec{\Omega} \end{bmatrix} \\ &\equiv \mathbf{A} \begin{bmatrix} \Delta\vec{\theta} - \Delta\vec{\theta}_{SET}^* \\ \vec{\Omega} \end{bmatrix} \end{aligned} \quad (115)$$

If \mathbf{Q} is a diagonal matrix of eigenvalues of \mathbf{A} , and Φ is the matrix of corresponding eigenvectors, then the transition matrix \mathbf{D} is

$$\mathbf{D}(\tau) = \Phi e^{\mathbf{Q}\tau} \Phi^{-1} \quad (116)$$

The derivative of \mathbf{D} is therefore

$$\frac{\partial \mathbf{D}}{\partial \tau} = \Phi \mathbf{Q} e^{\mathbf{Q}\tau} \Phi^{-1} = (\Phi \mathbf{Q} \Phi^{-1})(\Phi e^{\mathbf{Q}\tau} \Phi^{-1}) = \mathbf{A} \mathbf{D} \quad (117)$$

We apologise if these few notes seem incomplete, but we assure you that the remaining details in linearisation of \vec{f} (104) are quite straightforward. The only caveat is that with such a large number of terms, there are many opportunities for error in algebra and coding. Hence we always test linearisation code against numerical differentiation of \vec{f} . (In that case, one might say, why not just use the numerical derivatives, and dispense with all the extra analysis? The answer depends on whether you are more interested in saving analytical time or time waiting for a computer to respond.)

F Linearisation in terms of impulse energy

$\Delta\vec{P}$ can be eliminated in favour of $(\Delta E, \Delta\epsilon)$ by differentiating the expression for impulse energy (32). First rewrite it as

$$\begin{aligned} E &= \vec{P}^T \left[\vec{V}_a^- + \frac{1}{2} \Delta \vec{V}_a \right] \\ &= \vec{P}^T \mathbf{G}_a \left[\vec{\Omega}^- + \frac{1}{2} \Gamma_a \vec{P} \right] \end{aligned} \quad (118)$$

Differentiating leads to

$$dE = d\vec{P}^T \mathbf{G}_a [\vec{\Omega} + \Gamma_a \vec{P}] + \vec{P}^T \mathbf{G}_a d\vec{\Omega} + \vec{P}^T \left[d\mathbf{G}_a \left[\vec{\Omega} + \frac{1}{2} \Gamma_a \vec{P} \right] + \frac{1}{2} \mathbf{G}_a d\Gamma_a \vec{P} \right] \quad (119)$$

Now write \vec{P} as

$$\vec{P} = P \begin{bmatrix} \cos(\alpha + \epsilon) \\ \sin(\alpha + \epsilon) \end{bmatrix} \equiv P \vec{p} \quad (120)$$

Then the differential of \vec{P} is

$$d\vec{P} = dP \vec{p} + P d\vec{p} \quad (121)$$

To get dP , return to the energy formula (119). In terms of (P, \vec{p}) it becomes

$$dE = \vec{p}^T \mathbf{G}_a [\vec{\Omega} + \Gamma_a \vec{P}] dP + \vec{P}^T \mathbf{G}_a d\vec{\Omega} + \left[P \frac{\partial \vec{p}^T}{\partial \alpha} \mathbf{G}_a [\vec{\Omega} + \Gamma_a \vec{P}] + \vec{P}^T \left[\frac{d\mathbf{G}_a}{d\alpha} \left[\vec{\Omega} + \frac{1}{2} \Gamma_a \vec{P} \right] + \frac{1}{2} \mathbf{G}_a \frac{\partial \Gamma_a}{\partial \alpha} \vec{P} \right] \right] d\alpha + \frac{1}{2} \vec{p}^T \mathbf{G}_a \frac{\partial \Gamma_a}{\partial \theta_T} \vec{P} d\theta_T + P \frac{\partial \vec{p}^T}{\partial \epsilon} \mathbf{G}_a [\vec{\Omega} + \Gamma_a \vec{P}] d\epsilon \quad (122)$$

Solving for dP leaves an expression of the form

$$dP = \frac{\partial P}{\partial \alpha} d\alpha + \frac{\partial P}{\partial \theta_T} d\theta_T + \frac{\partial P}{\partial \vec{\Omega}} d\vec{\Omega} + \frac{\partial P}{\partial E} dE + \frac{\partial P}{\partial \epsilon} d\epsilon \quad (123)$$

Putting this into (121), and extending the expression for *finite* differences, leaves $\Delta \vec{P}_k$ in terms of (E_k, ϵ_k) , and the state variables at the start of step k . Then each term of the S-to-S linearisation must be modified. For example, from (107) and (110)

$$\frac{\partial \vec{f}_e}{\partial \alpha_k} = \frac{\partial \vec{f}}{\partial \alpha_k} + \frac{\partial \vec{f}}{\partial \vec{P}} \frac{\partial \vec{P}}{\partial \alpha} \quad (124)$$

Thus are the S-to-S equations converted from (43) to (44).

G Minimum time for impulse application

When a toe-off impulse is applied to the swing leg, an impulsive downward reaction is required on the stance foot to maintain contact with the ground. If walking is to continue, the reaction force must be kept smaller than the maximum available, *i.e.* the

weight of the machine. Therefore the impulse must be spread over some finite time interval. The minimum time can be estimated as follows. First note that the toe-off and reaction impulses must account for the total change in linear momentum on impulse application. Thus the reaction impulse is

$$\vec{P}_C = m_C \Delta \vec{V}_C + m_F \Delta \vec{V}_F + m_T \Delta \vec{V}_T - \vec{P} \quad (125)$$

According to (35), this can be written in terms of $\Delta \vec{\Omega}$ as

$$\vec{P}_C = (m_C \mathbf{G}_C + m_F \mathbf{G}_F + m_T \mathbf{G}_T) \Delta \vec{\Omega} - \vec{P} \quad (126)$$

$\Delta \vec{\Omega}$ in turn is a function of \vec{P} (35); hence

$$\vec{P}_C = [(m_C \mathbf{G}_C + m_F \mathbf{G}_F + m_T \mathbf{G}_T) \Gamma_a - \mathbf{I}] \vec{P} \quad (127)$$

If the impulse is delivered in an interval τ_P , then the reaction force will be

$$\vec{F}_C = \frac{\vec{P}_C}{\tau_P} \quad (128)$$

Thus the reaction force will be less than the weight provided that

$$1 + \frac{\vec{P}_{Cx}}{\tau_P} > 0 \quad (129)$$

As an example, take $m_H = 0.7$, $\gamma = -0.025$ from figure 15, for which

$$\vec{P}_0 = \begin{bmatrix} 0.134 \\ 0.042 \end{bmatrix} \quad (130)$$

$$[(m_C \mathbf{G}_C + m_F \mathbf{G}_F + m_T \mathbf{G}_T) \Gamma_a - \mathbf{I}] = \begin{bmatrix} -0.732 & -0.198 \\ 0.201 & 0.063 \end{bmatrix} \quad (131)$$

Then

$$\vec{P}_C = \begin{bmatrix} -0.106 \\ 0.029 \end{bmatrix} \quad (132)$$

The minimum-time condition (129) then becomes

$$\tau_P > 0.106 \quad (133)$$

which is 4% of the step period. While this is reasonably small, a more important measure of the interval is the movement of the point of application. An estimate is

$$\Delta \begin{bmatrix} x_a \\ y_a \end{bmatrix} \approx \mathbf{G}_a \vec{\Omega}^+ \tau_P = \begin{bmatrix} 0.013 \\ 0.017 \end{bmatrix} \quad (134)$$

Here we have used the *post-pulse* $\tilde{\Omega}$ in the calculation. A position shift of this size would call for rotation of the toe-off actuator by about $0.02rad$, which is significant – as comparison of figures 17 and 16 will attest. Hence our caveat that in practice the values of ϵ recommended by the steady-walking conditions (42) may have to be adjusted slightly.

References

- [Gabrielli 50] G. Gabrielli, T. von Karman. What Price Speed? *Mechanical engineering* 72(10) 1950.
- [Gibbs-Smith 70] C. Gibbs-Smith. *Aviation. An historical survey from its origins to the end of world war 2*. HMSO, 1970.
- [Lee 88] T-T. Li, J-H. Liao. Trajectory planning and control of a 3-link biped robot. *IEEE int. conf. robotics and automation*, Philadelphia, 1988.
- [McGeer 88] T. McGeer. Passive Dynamic Walking. Submitted to *Int. J. robotics research*. January 1988.
- [McMahon 84] T. McMahon. Mechanics of locomotion. *Int. J. robotics research* 3(2) 1984.
- [Mita 84] Mita, T. *et al.* Realisation of a high speed biped using modern control theory. *Int. J. control* 40(1) 1984.
- [Miura 84] H. Miura and I. Shimoyama. Dynamic walking of a biped. *Int. J. robotics research* 3(2) 1984.
- [Raibert 86] M. Raibert. *Legged robots that balance*. MIT Press, 1986.
- [Takanishi 85] A. Takanishi *et al.* The realisation of dynamic walking by the biped walking robot WL-10RD. *Int. conf. advanced robotics*, Tokyo 1985.
- [Yamada 85] M. Yamada *et al.* Dynamic control of a walking robot with kick action. *Int. conf. advanced robotics*, Tokyo 1985.
- [Zheng 88] Y.F. Zheng, J. Shen, and F. Sias. A motion control scheme for a biped robot to climb sloping surfaces. *IEEE int. conf. robotics and automation*, Philadelphia, 1988.

Figure 1 *A bipedal toy which walks passively down shallow inclines.*
(From [McMahon 84])

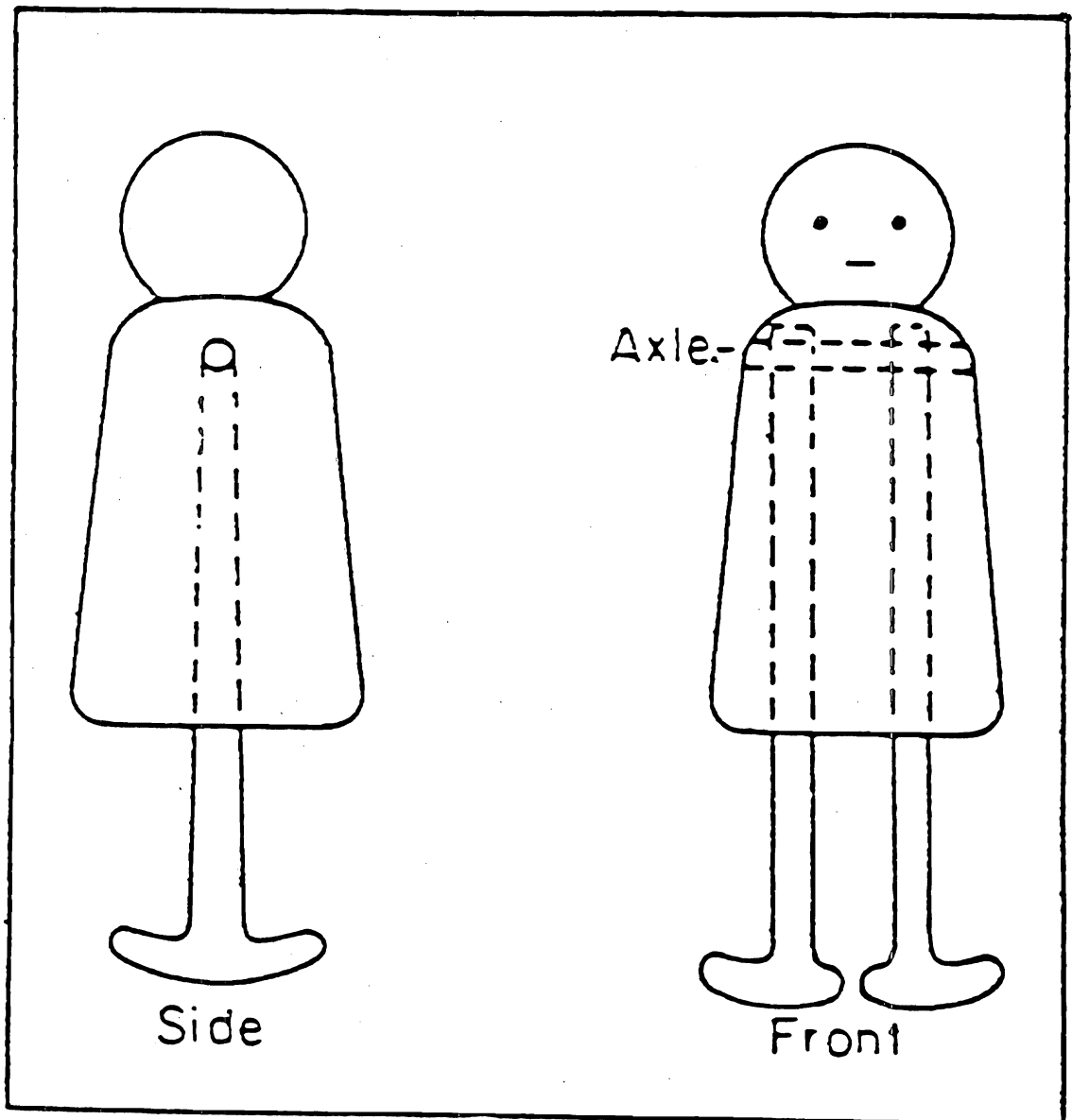
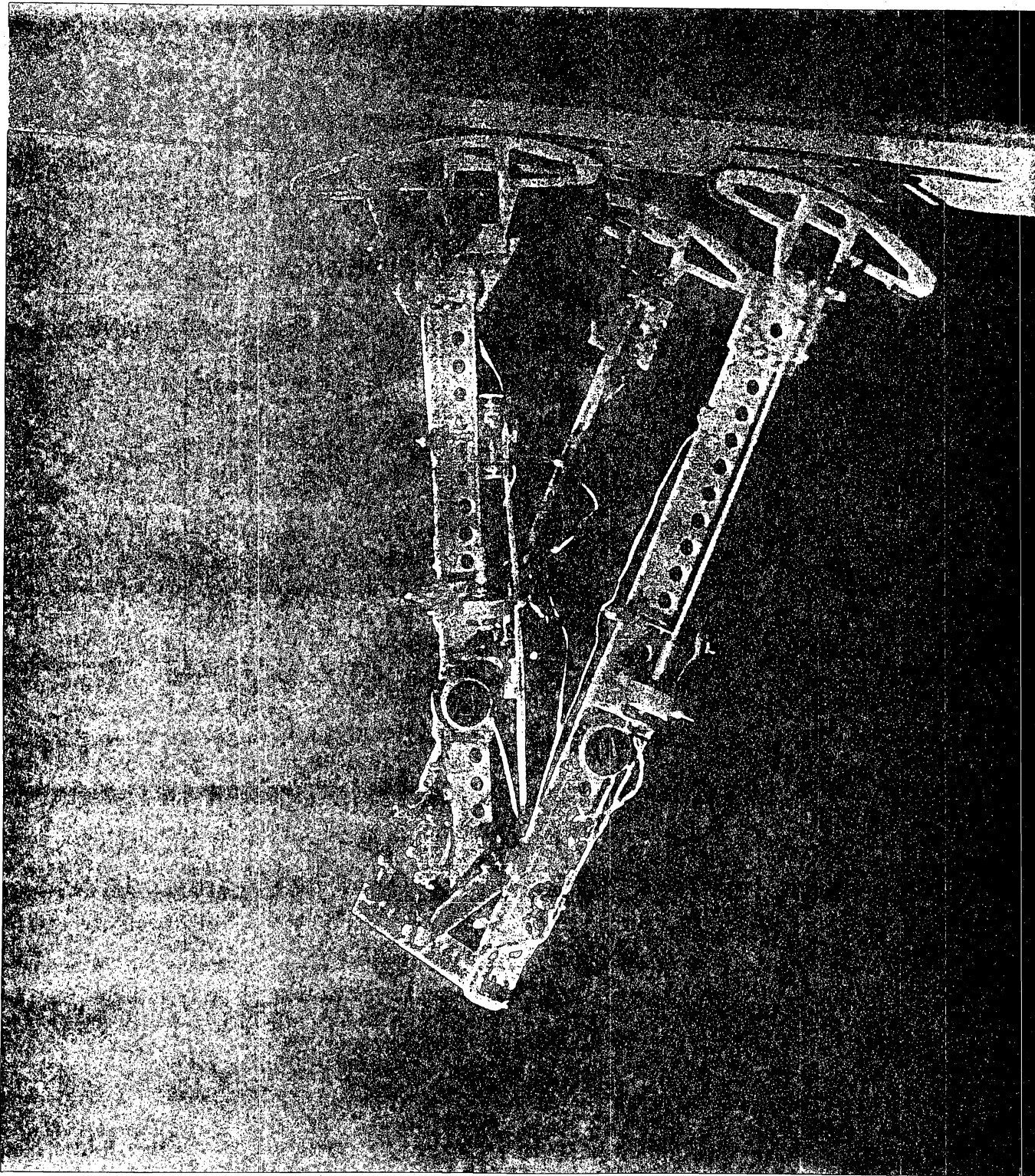


Figure 2 The biped used for experiments on two-dimensional gravity-powered walking. The outer legs are connected by a crossbar, and alternate like crutches with the centre leg. Toe-stubbing is prevented by small motors which retract the feet during the swing phase. Apart from that, this machine, like the toy, walks in a naturally stable limit cycle requiring no active control. Leg length is 50cm, and weight 9.5kg.



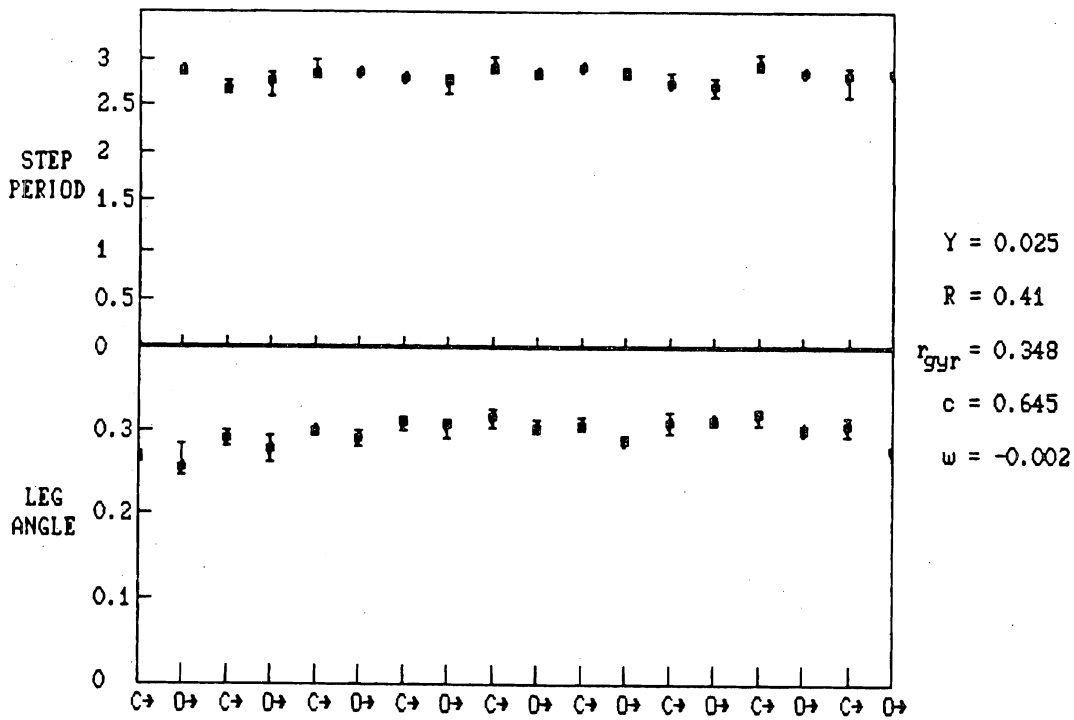


Figure 3 Step period and leg angle at heel strike (α , in rad.) in passive walking. The machine of figure 2 was started by hand on a 5.5m ramp inclined at 2.5% downhill, and after a few steps settled into a fairly steady gait. Dots show the mean values, and bars the scatter recorded over 5 trials. Lengths are made dimensionless by leg length l , and times by $\sqrt{l/g}$. "C" denotes start-of-stance on the centre leg; "O" on the outer legs.

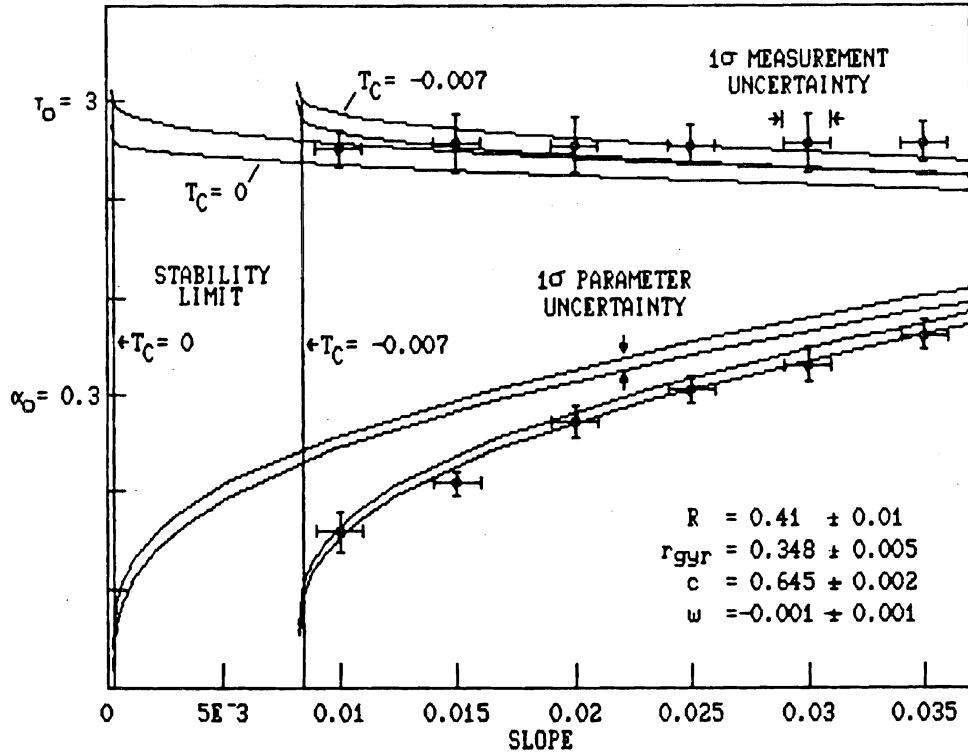


Figure 4 Stride angle α_0 and period τ_0 in passive walking of the machine of figure 2. 5 trials were done on each slope. Results from the first few steps of each trial were dropped, and the remaining data averaged. Bars show 1 standard deviation. Theoretical behaviour was calculated using the parameters of the test machine. These were measured with some uncertainty; the bands show the resulting uncertainty in expected performance. Reasonable consistency between model is measurement is realised if the rolling friction $-T_C$ is taken to be 0.007, which in dimensional terms is equivalent to 25gm-force applied at the hip joint. We could not measure the rolling friction independently, but this magnitude seems within the realm of possibility.

Figure 5 A "synthetic wheel." In its natural limit cycle it rolls like an ordinary wheel.
On each step the free leg swings forward to synthesize a continuous rim.

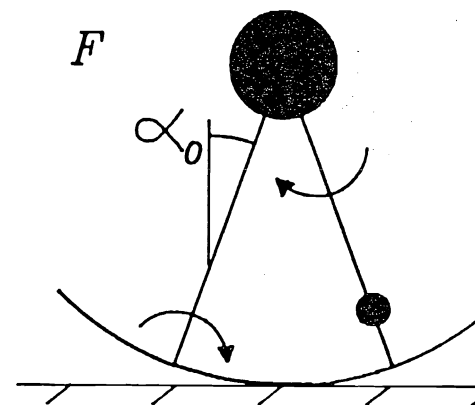
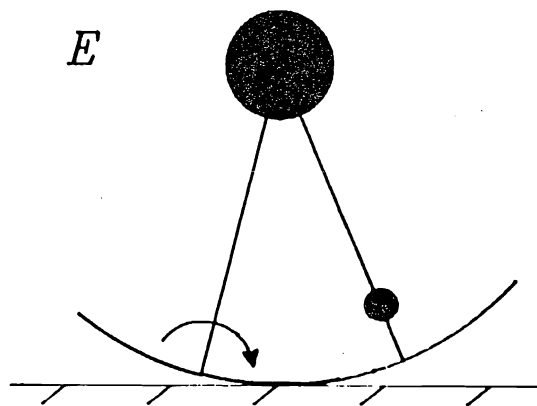
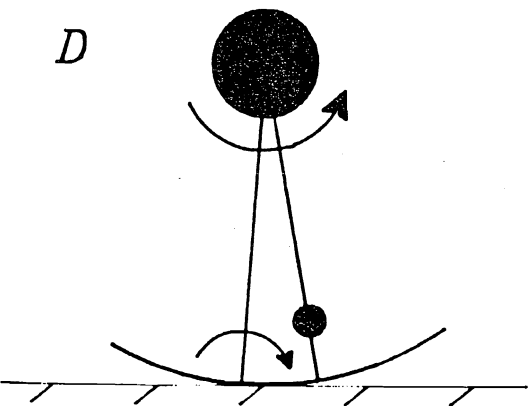
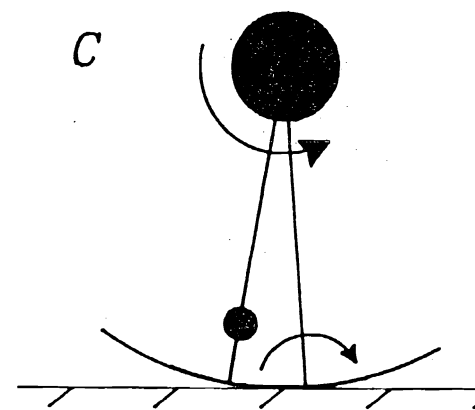
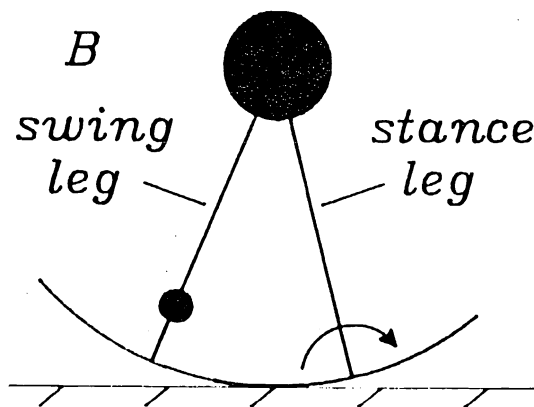
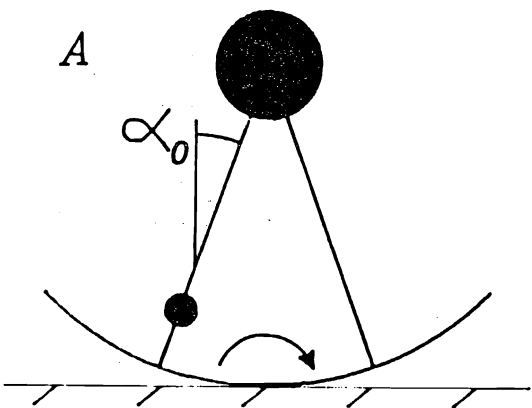
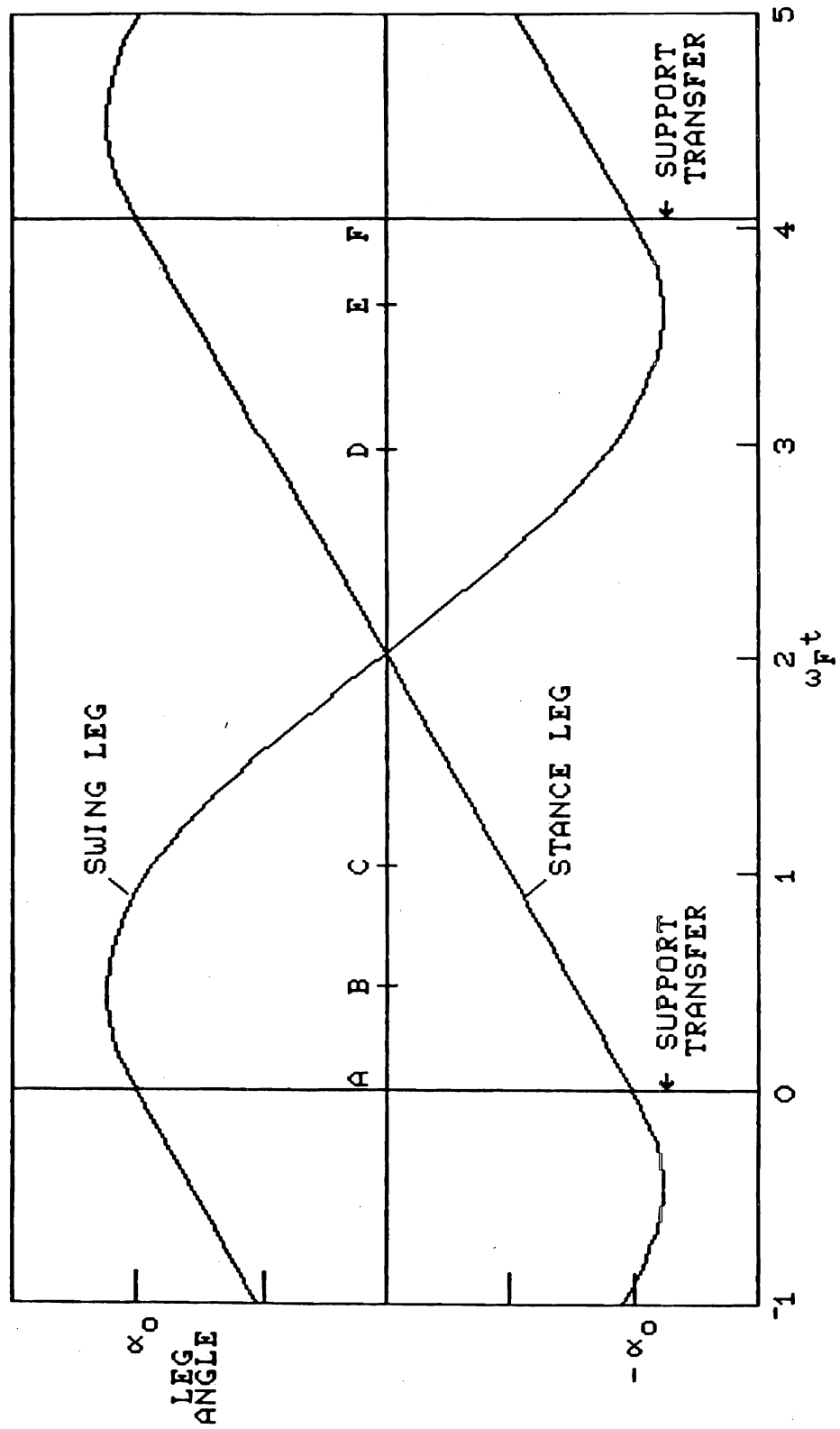


Figure 6 One step of a synthetic wheel. Points corresponding to the frames in figure 5 are indicated by letter. If support is transferred from trailing to leading leg when the angles are equal and opposite, then the walking cycle can continue without loss of energy. The period of the cycle (here non-dimensionalised by the pendulum frequency of the swing leg) is independent of the step length.



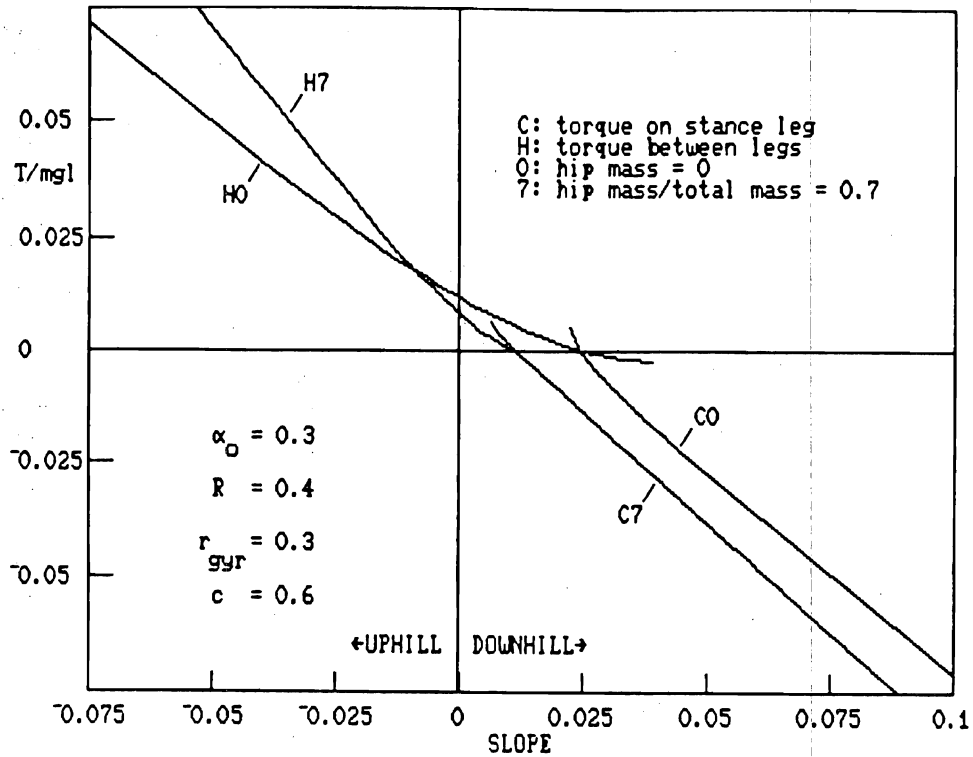


Figure 8 Energy can be exchanged with the walking mode by applying torque to the stance leg, or between legs at the hip joint. Thus any selected stride (here with $\alpha_0 = 0.3$) can be maintained over a range of slopes. If the torque is zero, then in the steady walk the energy gained in descent balances the energy dissipated on support transfer. Notice that less energy is dissipated with a "payload" at the hip than with the legs alone. A steeper descent requires a braking torque, proportional to the additional energy which has to be dissipated. Similarly, ascent requires some energy input. Stance and hip torque are effective in different regimes; this is further illuminated by figure 9.

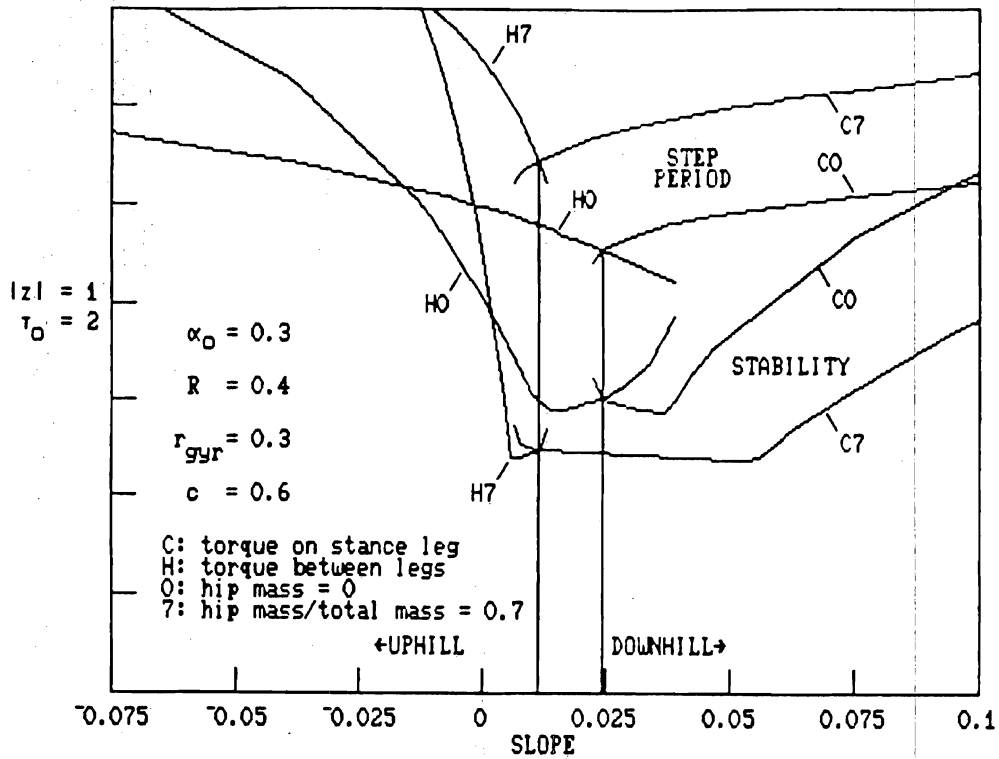


Figure 9 The range of slopes negotiable by torque-powered walking is limited at one end by complete vanishing of the walking cycle, and on the other by the cycle becoming unstable (indicated here by $|z| > 1$). Notice that while hip and stance torques are effective on different slopes, the range of acceptable step periods is the same for both torque strategies.

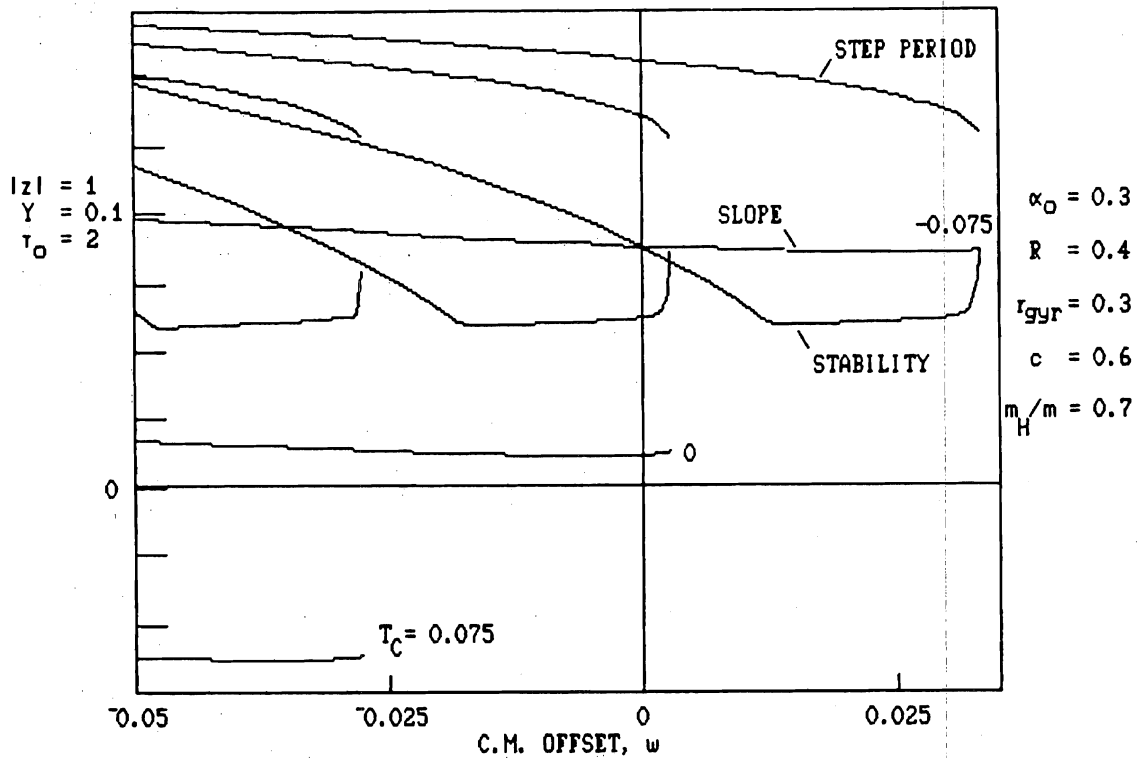


Figure 10 Figure 9 shows that if the legs' mass distribution is fixed, then steady walking is possible over only a limited range of slopes. However, this range can be shifted by changing the offset between the leg axes and mass centres. This example shows that a small backward offset of the mass centre accommodates positive stance torque with a reasonable step period, thus allowing stable uphill walking. Similarly a forward offset allows walking on steep downhill grades.

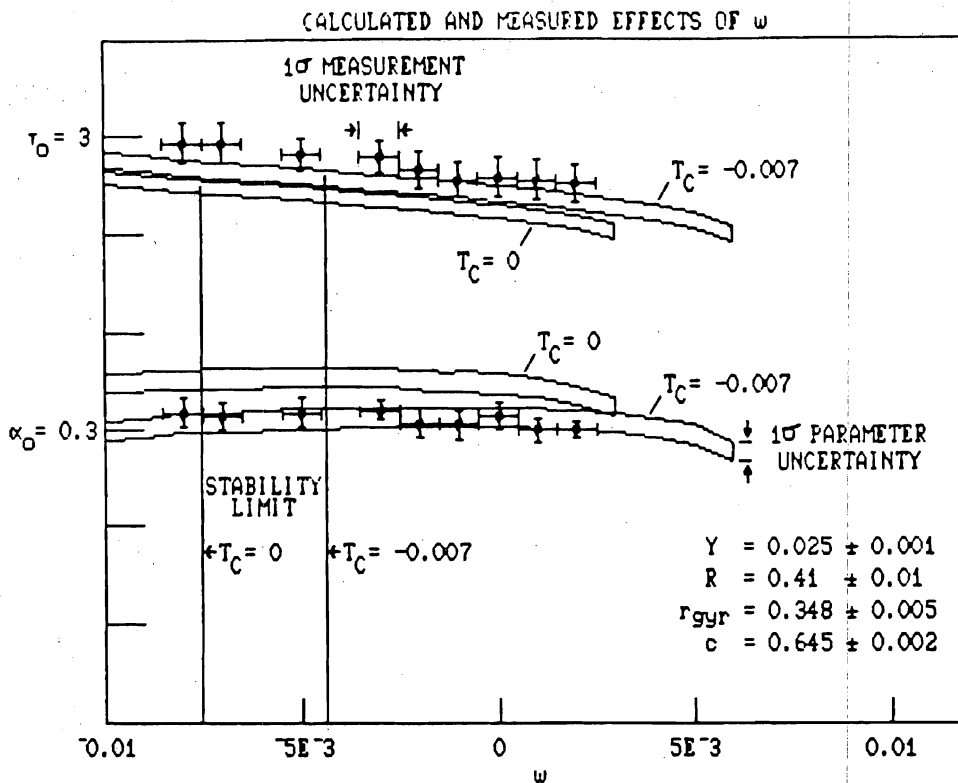


Figure 11 Experiments with our test machine confirmed the sensitivity of walking to offset of the legs' mass centres. w was adjusted by shifting the feet relative to the legs. With each setting we did several trials similar to those of figure 3. α_0 and τ_0 are well matched by calculations if T_C is taken to be -0.007 , but then walks which were in fact sustained for the full length of three 6-foot tables are calculated to be unstable. Taking T_C to be zero gives a better match to the observed stability, but leaves relatively large discrepancies in α_0 and τ_0 . Thus the model is not completely accurate, but it is correct in predicting that small changes in w have a large effect on step period.

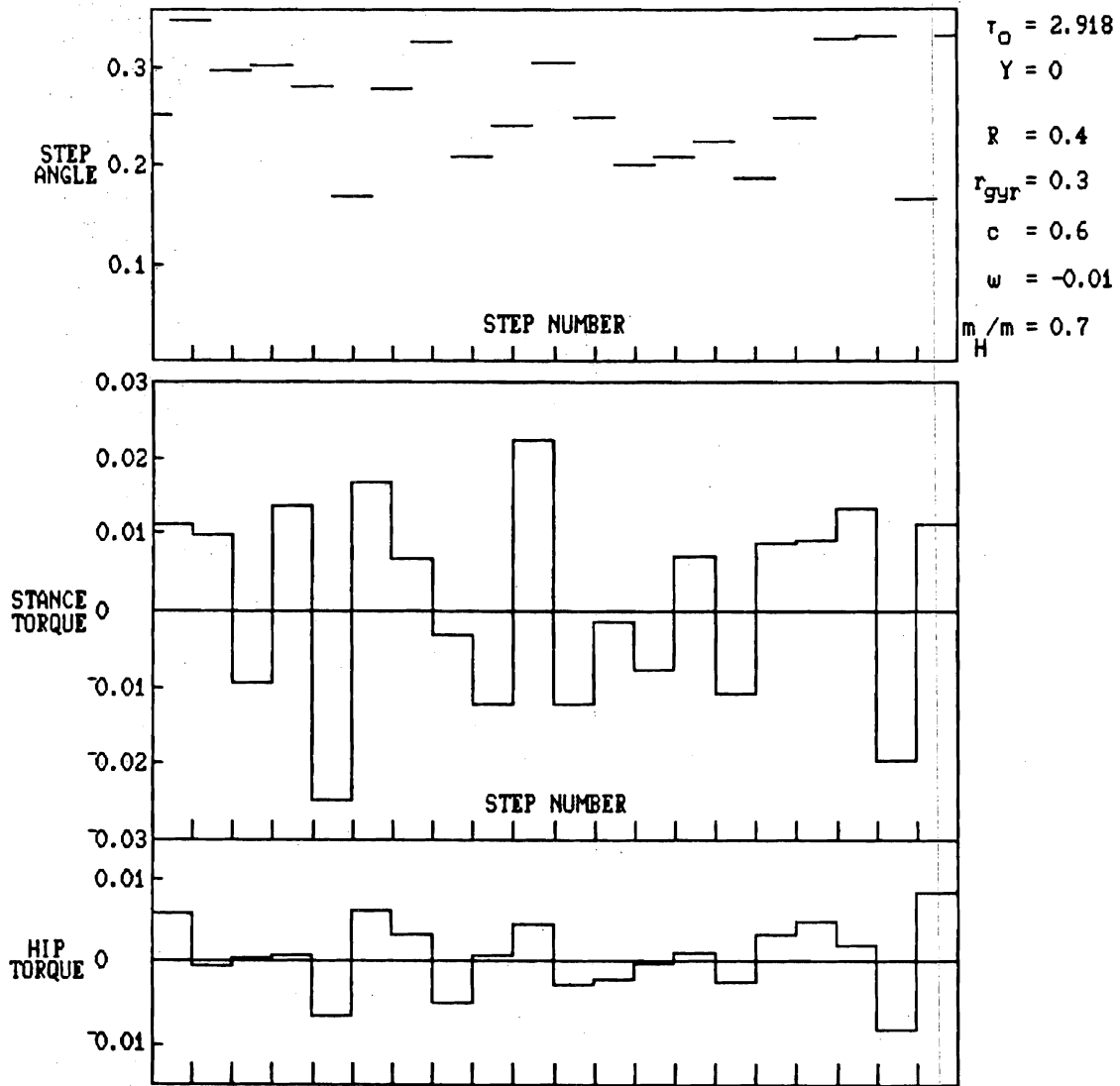


Figure 12 A practical biped must be capable of not only steady walking over a range of smooth slopes, but also walking where footholds are irregularly spaced. Here we imagine crossing a pond via a set of randomly-spaced stepping stones. With stance and hip torque as control variables, the machine can maintain a constant step period, while varying the step length from step to step. A similar control technique can be used for maintaining a steady gait over rolling terrain.

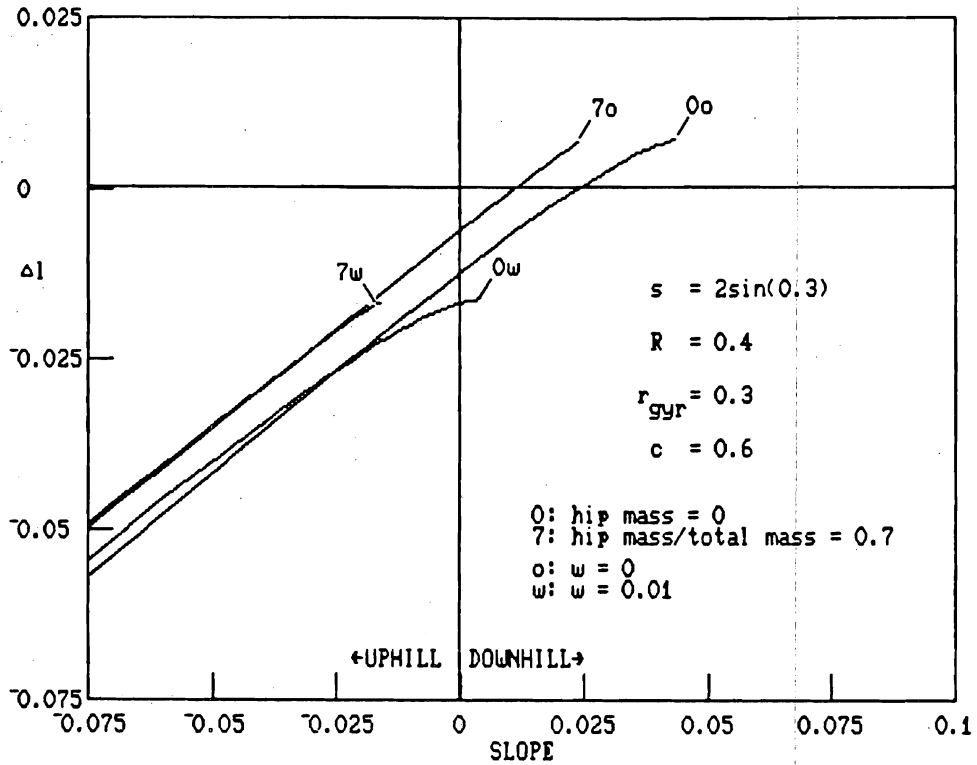


Figure 13 Another method of exchanging energy with the walking mode is leg length adjustment. If the swing leg is shortened during the step, then the machine will topple further prior to heel strike, and so convert the additional potential energy into kinetic energy at support transfer. Here α_0 is varied with Δl so that the same stride length is used on all slopes.

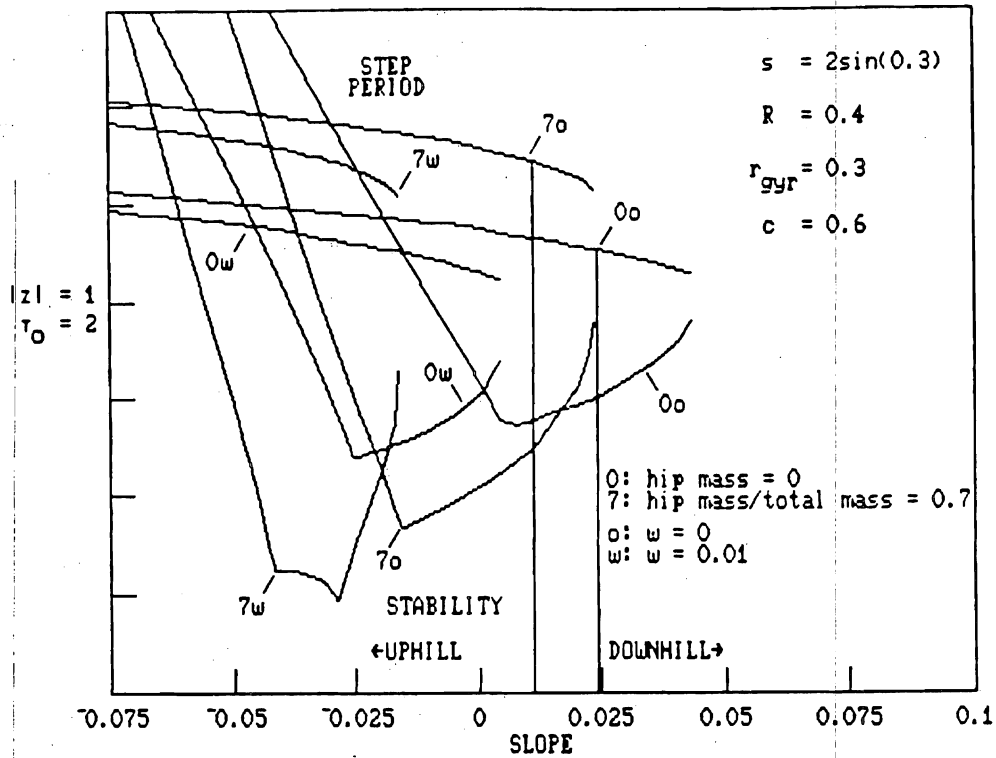


Figure 14 Length adjustment, like torque application, is effective for energy exchange only so long as the walking cycle exists and remains stable. As in figure 9 this is possible over only a limited range of step periods. The corresponding range of slopes can be adjusted by varying the offset between the leg axes and their mass centres.

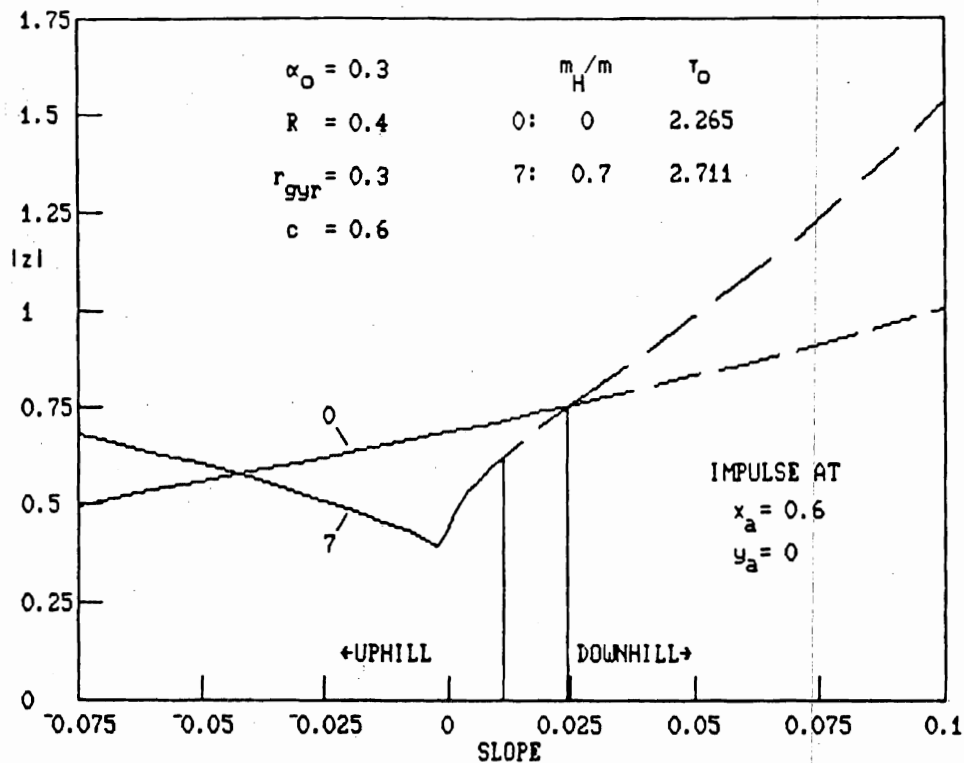


Figure 15 Yet another method for adding energy is to push with the trailing leg as it leaves the ground. Here the push is taken to be impulsive, and applied at the centre of curvature of the trailing foot. By appropriate choice of magnitude and direction of the impulse, the step period can be made independent of slope, and so stable walking can be achieved over a broad range of slopes. However, toe-off pulsing is effective only for climbing; descending would call for the trailing leg to pull rather than push on the ground.

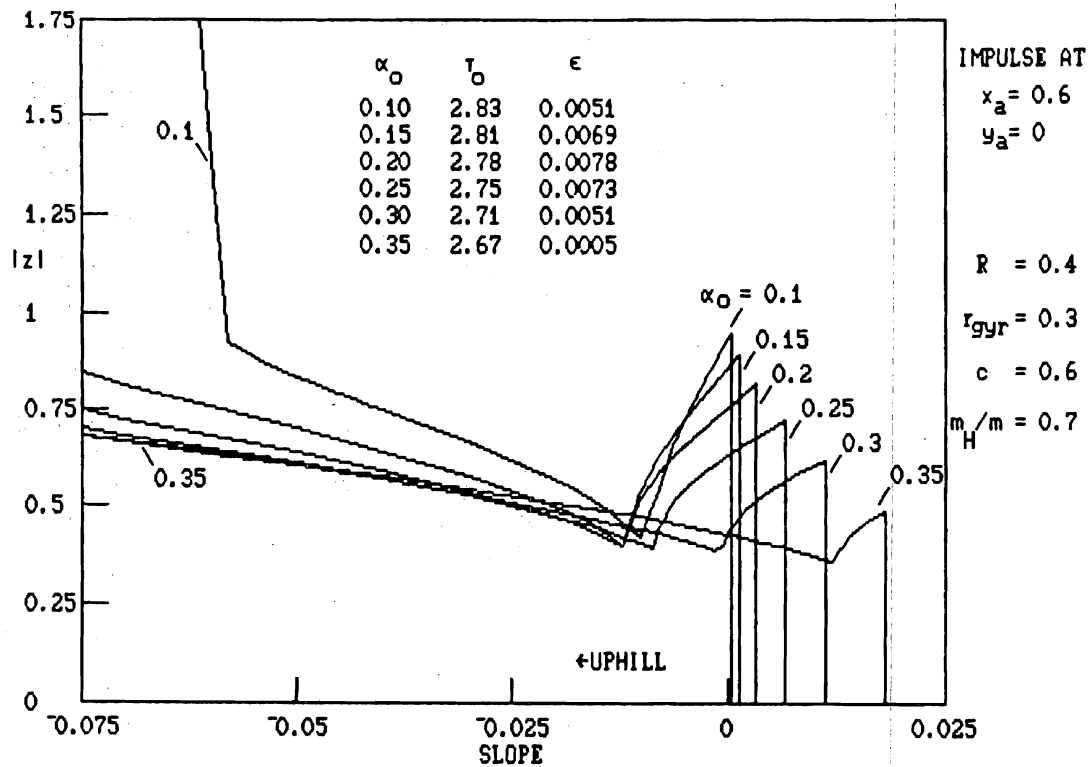


Figure 16 In practice one must be able to vary both slope and stride length. Toe-off pulsing allows a great deal of flexibility. These results show instability arising only in relatively steep climbs using a short stride. In fact this problem is more static than dynamic: even standing still becomes marginally stable with a small leg angle on a steep grade. The table gives the impulse-application angles which make the step period independent of slope, and the corresponding step periods. These indicate that the impulse should be nearly parallel to the trailing leg, with only a slight forward incline.

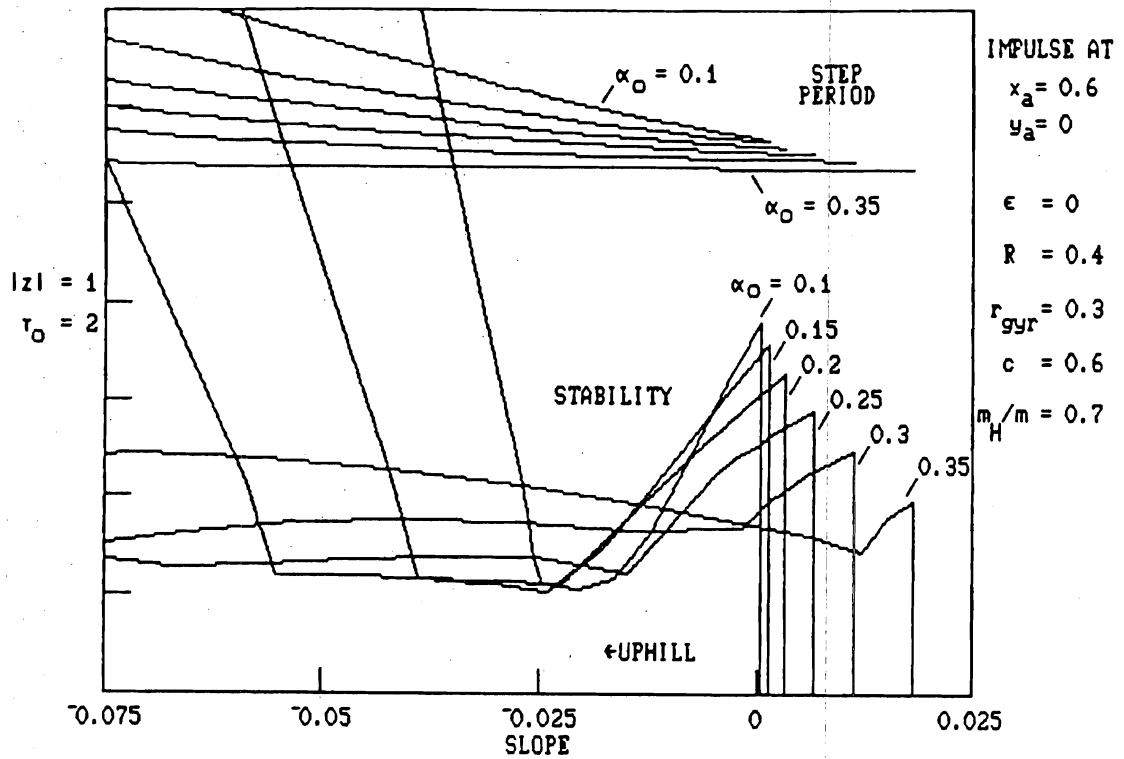


Figure 17 Since the data in figure 16 indicate that the toe-off impulse should be nearly parallel to the leg, it would seem practically reasonable to build the actuator exactly parallel to the leg. However, comparison of this plot with figure 16 reveals that only a few mrad in ϵ makes quite a difference to step period and stability. Thus ϵ must be adjusted with a great deal of care.

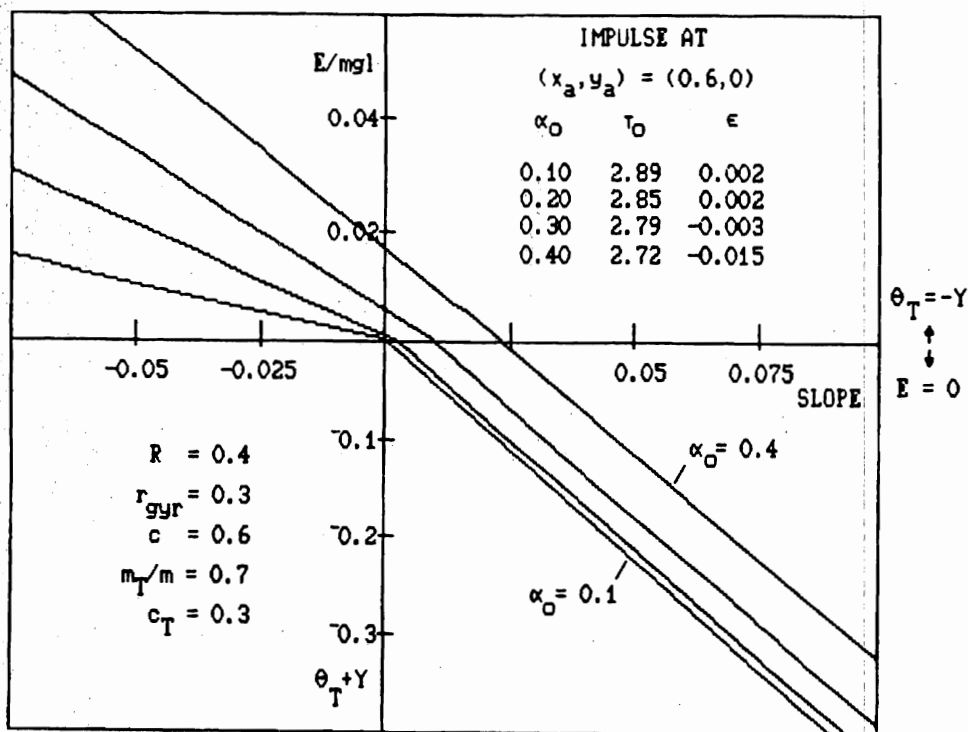


Figure 18 Since toe-off pulsing is effective only for climbing, a practical machine must have an alternative control for descending. One alternative is stance torque, which in this example is generated by reaction against a massive leaning torso. Thus a steep descent is maintained by leaning the torso backward, by as much as 0.4rad on a 10% grade. On more moderate grades the recline is less dramatic, so that the torso is exactly vertical ($\theta_T = -\gamma$) on some relatively shallow slope. Here we have specified that the torso remains vertical for uphill climbing, and an additional energy E is applied by a toe-off pulse. The pulse angle is chosen so that τ_0 is independent of slope. Note that E and θ_T are in no way comparable quantities; they are plotted on the same axis only because they are the appropriate control variables in the up- and downhill regimes.

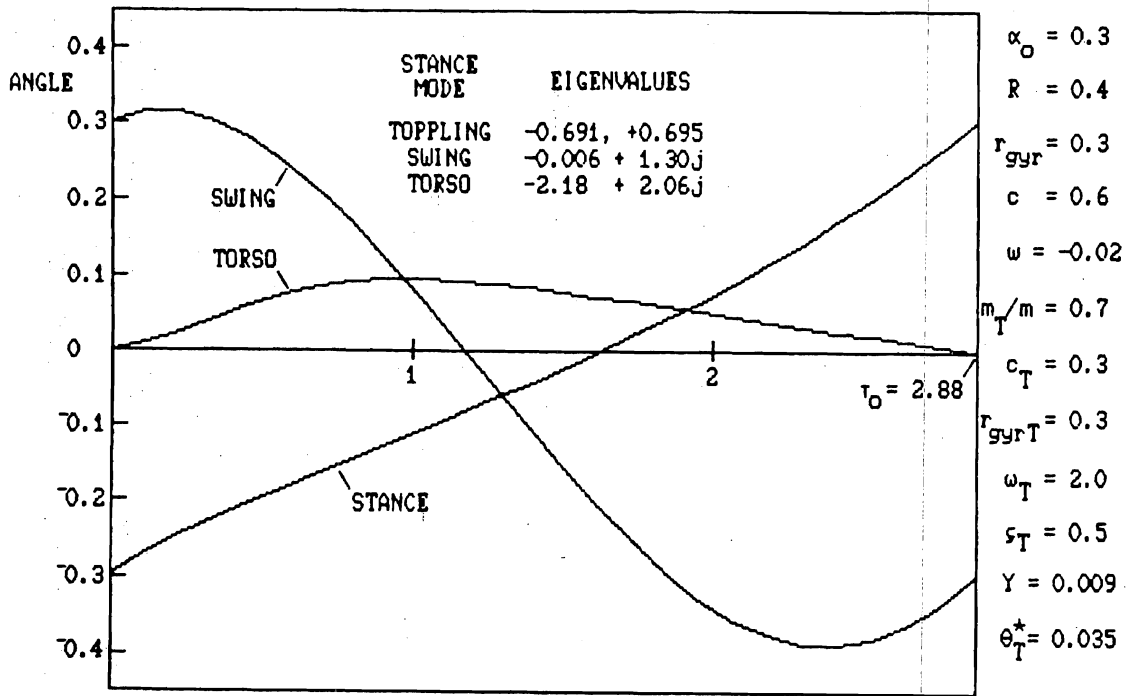


Figure 20 Figures 18 and 19 were calculated for perfect torso stabilisation, i.e. the torso angle remains constant throughout the step. In practice torso stabilisation will not be quite perfect. In this example the torso is taken to be stabilised by linear feedback, with closed-loop frequency roughly twice that of the swing mode. Thus at heel strike the torso is jerked forward, after which the controller slowly brakes the forward motion and brings the torso back to the vertical. This puts a positive torque on the stance leg, which would make the step period unacceptably small were it not for negative offset of the legs' mass centres ($w = -0.02$). (cf. figure 10)

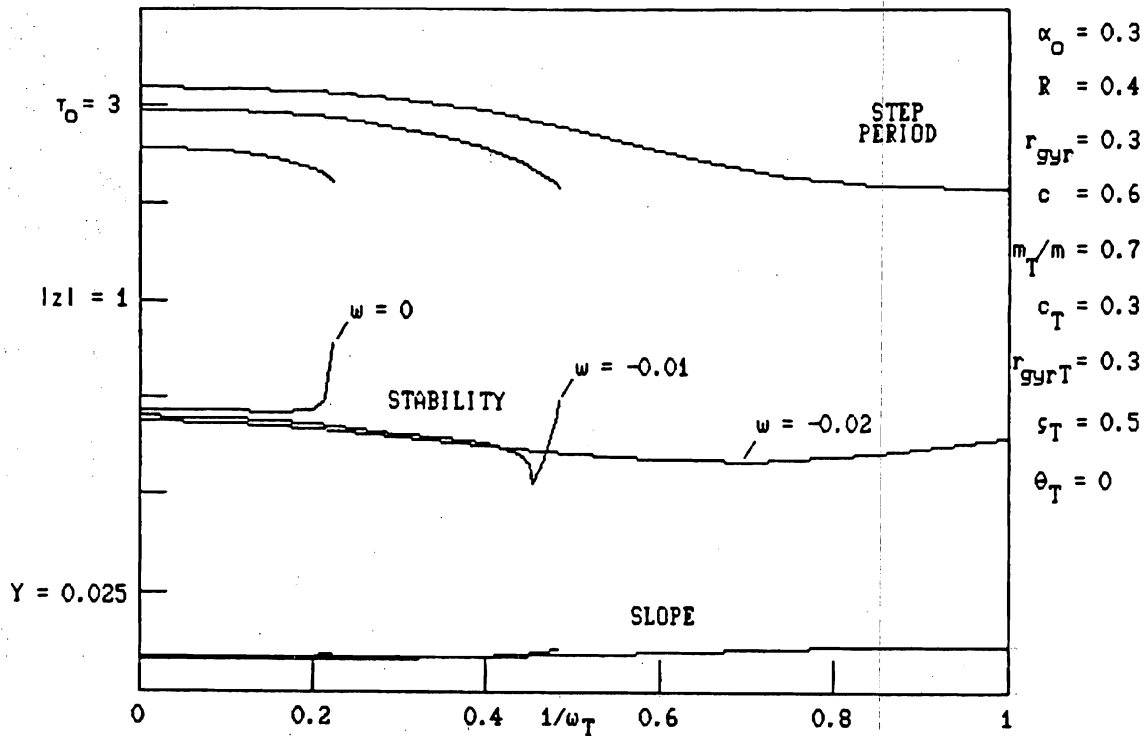


Figure 21 *Perfect torso stabilisation is most desirable, but the walking mode can remain intact even with quite soft control. The only caveat is that as the controller's timescale ($1/\omega_T$) increases, the leg's mass centres must be offset backward to maintain an acceptable step period.*

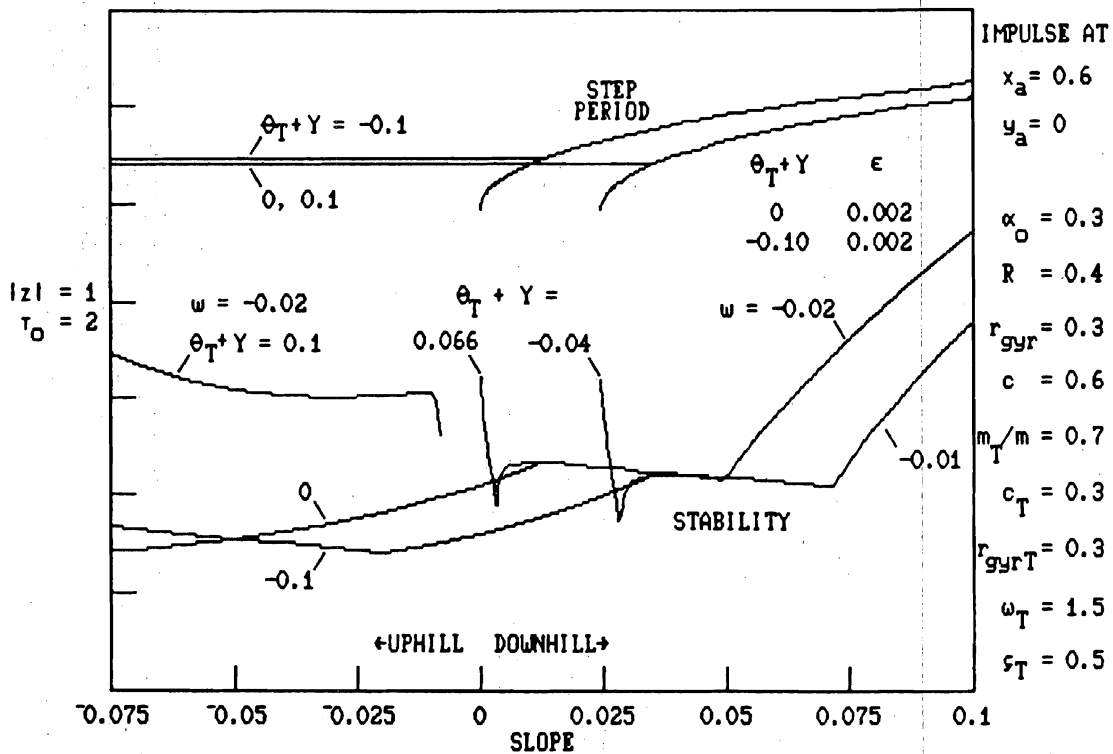


Figure 22 Provided that w is chosen appropriately, stability and step period calculated with a swaying torso are qualitatively similar to those calculated with perfect torso stabilisation (figure 19). In this example the torso controller is relatively slow. Variation of torso angle, toe-off impulse, and leg mass offset presents a very rich variety of options for stable walking.